Applied Mathematics and Computation 500 (2025) 129429

Contents lists available at ScienceDirect

Applied Mathematics and Computation

journal homepage: www.elsevier.com/locate/amc

Full Length Article

Symmetrised fractional variation with L^1 fidelity for signal denoising via Grünwald-Letnikov scheme

Alessandro Lanza [a], Antonio Leaci [b,*], Serena Morigi [a], Franco Tomarelli [c]

[a] Department of Mathematics, University of Bologna, Bologna, Italy
[b] Università del Salento, Dipartimento di Matematica e Fisica "Ennio De Giorgi", Lecce, Italy
[c] Politecnico di Milano, Dipartimento di Matematica, Italy

ARTICLE INFO

MSC:
26A33
26A45
49J45

Keywords:
Fractional variation
Total variation
Riemann-Liouville fractional derivatives
Grünwald-Letnikov scheme
Functions of bounded variation
Discretization of fractional derivatives
Calculus of variations
Abel equation
Signal analysis
Multi-parameter whiteness principle

ABSTRACT

We define, study and implement the model SFV-L^1: a variational approach to signal analysis exploiting the Riemann-Liouville (RL) fractional calculus. This model incorporates an L^1 fidelity term alongside fractional derivatives of the right and left RL operators to act as regularizers. This approach aims to achieve an orientation-independent protocol. The model is studied in the continuous setting and discretized in one dimension by means of a second-order consistent scheme based on approximating the RL fractional derivatives by a truncated Grünwald-Letnikov (GL) scheme. The discrete optimization problem is solved using an iterative approach based on the alternating direction method of multipliers, with guaranteed convergence.
A multi-parameter whiteness criterion is introduced which provides automatic and simultaneous selection of the two free parameters in the model, namely the fractional order of differentiation and the regularization parameter. Numerical experiments on one-dimensional signals are presented which show how the proposed model holds the potential to achieve good quality results for denoising signals corrupted by additive Laplace noise.

1. Introduction

Variational methods have been a cornerstone of signal and image processing for many years, as evidenced by their extensive presence in scientific literature. A general (deterministic) variational approach is expressed as the minimization of a cost functional under suitable constraints. The cost functional represents the overall "goodness" of competitors and is a combination of two key terms: a fitting data term which measures the discrepancy between the observed data (the "ground truth") and the sought solution, say it reflects how well our solution matches the actual data; a regularizing term which incorporates prior knowledge or assumptions about the desired solution.

The regularizing term plays a crucial role in several ways: it can help stabilize ill-posed problems, where there may be multiple possible solutions or none at all.

The regularizer helps guide us towards the most desirable solution based on our prior knowledge. It ensures the overall cost functional has desirable mathematical properties (coercivity and lower semicontinuity) for specific topologies.

* Corresponding author.
E-mail addresses: alessandro.lanza2@unibo.it (A. Lanza), antonio.leaci@unisalento.it (A. Leaci), serena.morigi@unibo.it (S. Morigi), franco.tomarelli@polimi.it (F. Tomarelli).

https://doi.org/10.1016/j.amc.2025.129429
Received 27 June 2024; Received in revised form 10 January 2025; Accepted 23 March 2025

Available online 1 April 2025

These properties are essential for applying powerful optimization techniques from the calculus of variations.

Classical nonconvex variational models are the Mumford-Shah and Blake-Zisserman ones ([16], [23]) which were extensively used in image segmentation and denoising. Another classical model for image analysis is the Rudin-Osher-Fatemi model [47] also known as ROF or TV (total variation), which is based on a convex minimization, and has several variations in the literature [21,44,51]: in such model, the regularizing term is a first order term, namely the total variation that turns to be the ℓ^1 norm of the gradient in a discretized setting. To avoid artifacts as staircasing which appears in TV approach, the total variation term has been modified in some cases by adding second order derivatives, see e.g. the Total Generalized Variation (TGV) in [9], and by extending to fractional TV-norm, as in [38]. Similar models have been developed with different second order terms for denoising in [27] or segmentation and inpainting as in [12–18].

In all these models the regularization term adopts integer-order derivatives. To take advantage of nonlocal properties of fractional derivatives, some fractional order TV-like models have been proposed for signal denoising [19,44,45,37]. However, these approaches deal mainly with the finite dimensional framework (after discretization) and few among them propose an infinite dimensional approach together with a suitable mathematical analysis ([34,35]). We mention also the work by Zhang and Chen [51] which provides an anisotropic total fractional-order variation model for image restoration in a continuous setting, and Golbaghi et al. in [28] that introduced a variable-order total fractional variation model in a suitable normed space $BV^{s(x)}$.

In [35] we introduced and analyzed an isotropic Fractional Variation model with fidelity term in L^2, namely the minimization of the functional

$$\mathcal{F}(u) \;:=\; \frac{\lambda}{2}\int_0^1 |u(x)-g(x)|^2\,dx \;+\; \|D_+^s[u]\|_{T_+} \;+\; \|D_-^s[u]\|_{T_-}\;, \tag{1.1}$$

where: $0<s<1$; $\lambda>0$ is the regularization parameter; g is a given noisy signal; D_+^s and D_-^s are the Riemann-Liouville left and right derivatives; $\|\cdot\|_{T_+}$ and $\|\cdot\|_{T_-}$ respectively denote the total variation in $[0,1)$ and $(0,1]$, see (3.2) and (3.3).

When using a variational model like (1.1) for signal denoising, it is well-known that the "optimal" functional form of the fidelity term is strictly related to the statistics of the noise corruption, according to the Maximum Likelihood estimation approach. In particular, the L^2 fidelity term in (1.1) corresponds to the assumption that data are corrupted by additive white Gaussian noise. The variant of using an L^1 fidelity term in standard ROF model was introduced in the context of image denoising and deblurring by Alliney and Nikolova [1,39,40]. In [39] Nikolova shows that for certain types of noise the regularization with L^1 fidelity outperforms the standard model. In particular, the L^1 fidelity is optimal for additive white Laplace noise and performs very well, in general, for noises of impulsive type, usually due to transmission errors or malfunctioning elements in acquisition sensors. In the present paper we introduce and study a Symmetrised Fractional Variational model with fidelity term in L^1: the model (shortly denoted as SFV-L^1) is based on minimality of fractional variation for restored images: a suitably weighted fidelity term matches with a regularizing term corresponding to the sum of total variations of both left and right fractional derivatives:

$$\mathcal{G}(u) \;:=\; \lambda\int_0^1 |u(x)-g(x)|\,dx \;+\; \|D_+^s[u]\|_{T_+} \;+\; \|D_-^s[u]\|_{T_-}\;. \tag{1.2}$$

An essential tool in the analysis of this variational model is a compactness property of fractional bounded variation spaces BV^s proved in [34] and recalled here in Theorem 2.6. Both the L^1 and L^2 fidelity terms lead to existence of minimizers that belongs to the space BV^s defined in [33], [34]. While the L^2 fidelity term leads to uniqueness of solution, the L^1 fidelity term may lack this property (see Remark 3.6 and Example 3.7). Moreover the L^1 fidelity term makes the whole functional $\mathcal{G}$ 1-homogeneous and hence fulfilling contrast equivariance (see Corollary 3.5).

The one dimensional case is considered in Sections 3, precisely the minimization problem related to the functional $\mathcal{G}$ as defined in (1.2), while the two dimensional formulation and study is postponed to a forthcoming paper [29]. We emphasize that, as long as fractional derivatives are involved, the symmetry is not warranted but must be imposed, since both right and left derivatives have different nontrivial kernels (see [35]). For this reason we consider a symmetrized approach to fractional variation (previously called bilateral fractional variation in the 1d framework [33]), with a regularizing filtering based on both left and right derivatives: namely functional $\mathcal{G}$ above and related optimization problem $\mathcal{P}_{\mathcal{G}}$ (see Section 3) which fulfills symmetry, since it depends on both left and right fractional derivatives.

About recent results concerning fractional Sobolev and fractional Bounded Variation spaces based either on Riemann-Liouville fractional derivatives or Gagliardo-type fractional Sobolev spaces we mention also [3,11,22,25,33,34]; denoising models with L^1 fidelity has been considered by [4,5,20] but coupled with fractional total variation filtering related to Gagliardo seminorms.

The advantages of using fractional TV regularization models like (1.1) and (1.2) come together with the issue of selecting a suitable value for the fractional-order parameter s, beyond the usual regularization parameter λ. In fact, it is well-known that even a very well-designed variational model can yield unsatisfactory results if the free model parameters are not properly set. Moreover, the larger the number of model parameters, the more difficult it is to use an empirical approach for their selection. In signal denoising, some criteria have been proposed in literature for automatically selecting a single parameter entering linearly the model (like λ in (1.1) and (1.2)), such as, e.g., the discrepancy principle, the L-curve and the generalized cross-validation criteria. More recently, the so-called Residual Whiteness Principle (RWP) has been introduced and proved to outperform the above-mentioned approaches [31,32]. In this paper, we apply a Multi-parameter RWP (MRWP) for the automatic and effective joint selection of the pair (s,λ) of free parameters in our model (1.2).

The proposed model (1.2) corresponds to an energy minimization in the symmetrized fractional bounded variation space BV^s introduced in [34]: this framework allows us to discretize the Riemann-Liouville fractional derivatives by means of a second-order consistent scheme based on a suitable truncated Grünwald-Letnikov scheme [42,41,49]. The achieved finite-dimensional minimization problem is then solved via an efficient iterative algorithm based on the Alternating Direction Method of Multipliers (ADMM) [8], with guaranteed convergence.

Some numerical experiments are presented which validate the proposed (discretized) model applied to denoising a set of representative one-dimensional signals characterized by different properties (namely, different regularities), ranging from piecewise affine signals to piecewise constant and smooth signals. The introduced MRWP parameter selection approach is also tested on the same denoising examples. The results indicate that values $s < 1$ of the fractional-order parameter are optimal for the complex signal whereas $s \approx 1$ and $s > 1$ are the best choices for the piecewise constant and smooth signal, respectively. The functional analysis theory of model (1.2) together with related computational simulations for general real parameter $s \geq 1$ and extension to the case of two dimensional images are postponed to a forthcoming paper [29]: the main challenges in these extensions rely on the achievement of suitable interpolation estimates when $s > 1$ and the definition of fractional partial derivatives by slicing in the 2d case.

2. Preliminary tools

We recall the definitions concerning classical Riemann-Liouville fractional calculus and some results useful in the sequel ([48]); for additional details about the bilateral approach we refer to [33,34].
The domain of a 1d signal could be any bounded interval (α, β) of $\mathbb{R}$; however, here and in the whole paper, we set $\alpha = 0$ and $\beta = 1$ for simplicity and without loss of generality. All along this paper we set $\mathbb{R}_+ = \{x \in \mathbb{R} : x \geq 0\}$ and $\mathbb{R}_{++} = \mathbb{R}_+ \setminus \{0\}$.
We denote the classical derivative by d/dx and the distributional derivative by D_x (or D). The symbol $W^{1,1}(0,1)$ represents the Sobolev space $\{u \in L^1(0,1) \mid Du \in L^1(0,1)\}$.

Definition 2.1. For every $0 < s < 1$ and $u \in L^1(0,1)$, the left-side and right-side Riemann-Liouville fractional integrals are defined respectively by

$$I_+^s[u](x) := \frac{1}{\Gamma(s)} \int_0^x \frac{u(t)}{(x-t)^{1-s}} dt \qquad 0 \leq x \leq 1, \tag{2.1}$$

$$I_-^s[u](x) := \frac{1}{\Gamma(s)} \int_x^1 \frac{u(t)}{(t-x)^{1-s}} dt \qquad 0 \leq x \leq 1.$$

Γ denotes the Gamma function here and in the sequel.

Definition 2.2 *(Distributional RL fractional derivative).* Assuming u in $L^1(0,1)$ and $0 < s < 1$, and, referring to [33], [34], the left and right Riemann-Liouville distributional derivatives of order s of u are given by

$$D_+^s[u](x) = D_x \left(I_{0+}^{1-s}[u] \right)(x) = \frac{1}{\Gamma(1-s)} D_x \int_{-\infty}^x \frac{u(t)}{(x-t)^s} dt \quad \text{on } (-\infty, 1), \tag{2.2}$$

$$D_-^s[u](x) := -D_x \left(I_{1-}^{1-s}[u] \right)(x) = \frac{-1}{\Gamma(1-s)} D_x \int_x^{+\infty} \frac{u(t)}{(t-x)^s} dt \quad \text{on } (0, +\infty). \tag{2.3}$$

Note that, referring to the trivial extension of u ($u = 0$ a.e. on $\mathbb{R} \setminus (0,1)$), all integrals in (2.1)-(2.3) are convolutions, though we consider their values restricted to the open set $(0,1)$ (see [33], [34]):

$$I_+^s[u](x) = u * \frac{H(x)}{\Gamma(s)|x|^{1-s}} = \frac{1}{\Gamma(s)} \int_0^1 \frac{u(t)\, H(x-t)}{|x-t|^{1-s}} dt \quad x \in \mathbb{R}, \tag{2.4}$$

$$I_-^s[u](x) = u * \frac{H(-x)}{\Gamma(s)|x|^{1-s}} = \frac{1}{\Gamma(s)} \int_0^1 \frac{u(t)\, H(t-x)}{|x-t|^{1-s}} dt \quad x \in \mathbb{R}. \tag{2.5}$$

Note that all the derivatives appearing in (2.2), (2.3) have to be understood in the distributional sense on the whole real line, thus $D_+^s[u]$ may have atomic part at $x = 0$ and $D_-^s[u]$ may have atomic part at $x = 1$ (see [34]).

Definition 2.3 *(RL fractional Sobolev spaces).* For $0 < s < 1$ set:

$$W_+^{s,1}(0,1) := \{w \in L^1(0,1) \mid I_+^{1-s}[w] \in W^{1,1}(0,1)\},$$

$$W^{s,1}_{-}(0,1) := \{ w \in L^1(0,1) \mid I^{1-s}_{-}[w] \in W^{1,1}(0,1) \}\,.$$

$W^{s,1}_{+}$ and $W^{s,1}_{-}$ are Banach spaces with their natural norms. Unfortunately the bounded subsets of $W^{s,1}_{+}$ and $W^{s,1}_{-}$ miss the L^1 compactness properties of their fractional derivatives. For this reason we introduced the fractional bounded variation counterparts of these spaces in [33,34].

Definition 2.4 *(RL fractional bounded variation spaces).* For every $s \in (0,1)$ the space $BV^s(0,1)$, sometimes shortly denoted BV^s, is

$$BV^s \;=\; BV^s_{+} \cap BV^s_{-}\,,$$

where

$$BV^s_{+} \;=\; \{ v \in L^1(0,1) \mid D^s_{+}[v] \in \mathcal{M}(0,1) \} \;=\; \{ v \in L^1(0,1) \mid I^{1-s}_{+}[v] \in BV(0,1) \}\,,$$
$$BV^s_{-} \;=\; \{ v \in L^1(0,1) \mid D^s_{-}[v] \in \mathcal{M}(0,1) \} \;=\; \{ v \in L^1(0,1) \mid I^{1-s}_{-}[v] \in BV(0,1) \}\,.$$

Here $\mathcal{M}(0,1)$ denotes the space of finite Radon measures:

$$\mathcal{M}(0,1) \;=\; \left\{ \mu \;\text{ s.t. }\; \|\mu\|_{\mathcal{M}(0,1)} := \sup_{\varphi \in C^0_0(0,1),\, |\varphi| \le 1} \int \varphi \, d\mu < +\infty \right\}.$$

For reader's convenience we recall two Theorems, proved in [34], showing that BV^s is a Banach space when provided with its natural norm and a suitable compactness of the bounded subsets of BV^s.

Theorem 2.5. *If $0<s<1$ then $BV^s(0,1)$ is a Banach space with the natural norm*

$$\|v\|_{BV^s(0,1)} \;:=\; \|v\|_{L^1(0,1)} + \| D^s_{+}[v] \|_{\mathcal{M}(0,1)} + \| D^s_{-}[v] \|_{\mathcal{M}(0,1)}\,.$$

For any given $p \in [1, 1/(1-s))$, there exists $C = C(s,p)$, s.t.

$$\|v\|_{L^p(0,1)} \le C(s,p)\, \|v\|_{BV^s(0,1)}.$$

Any function $v \in BV^s(0,1)$ can be represented by either one of these two formulas:

$$v(x) \;=\; I^s_{+}\big[D^s_{+}[v]\big](x) + \frac{I^{1-s}_{+}[v](0_+)}{\Gamma(s)}\, x^{s-1} \qquad a.e\ (0,1),$$
$$v(x) \;=\; I^s_{-}\big[D^s_{-}[v]\big](x) + \frac{I^{1-s}_{-}[v](1_-)}{\Gamma(s)}\, (1-x)^{s-1} \qquad a.e.\ (0,1).$$

Theorem 2.6 *(Compactness in $BV^s(0,1)$). Assume that $0<s<1$ and*

$$\|v_n\|_{BV^s(0,1)} \le C\,.$$

Then, there is v in $L^1(0,1)$ such that, up to subsequences,

$$\begin{cases} (i) & v_n \rightharpoonup v & w\text{-}L^p(0,1)\,, \quad \forall p \in [1, 1/(1-s))\,, \\ (ii) & I^{1-s}_{+}[v_n] \to I^{1-s}_{+}[v] & L^r(0,1)\ \forall r < +\infty\,, \\ (iii) & I^{1-s}_{-}[v_n] \to I^{1-s}_{-}[v] & L^r(0,1)\ \forall r < +\infty\,, \\ (iv) & I^{1-s}_{+}[v_n] \rightharpoonup I^{1-s}_{+}[v]\,, \quad I^{1-s}_{-}[v_n] \rightharpoonup I^{1-s}_{-}[v] & w\text{-}BV(0,1). \end{cases}$$

3. SFV-L^1: symmetrized fractional variation with L^1 fidelity term (1d)

In this section we introduce an approach for one dimensional signal restoration, based on Symmetrised Fractional Variation: namely, the minimization of a functional containing a data-fitting term balanced by a regularizing term expressed as the total variation of two-sided fractional derivatives.
Given

$$\lambda \in \mathbb{R}_{++}\,, \qquad s \in (0,1)\,, \qquad g \in L^1(0,1),$$

we study the problem

$$\min\ \{\, \mathcal{G}(u) :\ u \in BV^s(0,1) \} \tag{$\mathcal{P}_{\mathcal{G}}$}$$

where

$$\mathcal{G}(u) \;:=\; \|D^s_+[u]\|_{T_+} \,+\, \|D^s_-[u]\|_{T_-} + \lambda \int_0^1 |u(x)-g(x)|\,dx\,. \tag{3.1}$$

With λ indicating the so-called regularization parameter for the L^1 fitting term, s is the fractional order of the derivatives and g is the measured datum. Furthermore $D^s_+[u]$ and $D^s_-[u]$ denote respectively the left and right distributional RL fractional derivatives of u, thus $D^s_+[u]\equiv 0$ on $(-\infty,0)$ and $D^s_-[u]\equiv 0$ on $(1,+\infty)$; precisely we set

$$\|D^s_+[v]\|_{T_+} \;:=\; \|D^s_+[v]\|_{\mathcal{M}(0,1)} + |I^{1-s}_+[v](0_+)| \;=\; \|D^s_+[v]\|_{\mathcal{M}(-\infty,1)}\,, \tag{3.2}$$

$$\|D^s_-[v]\|_{T_-} \;:=\; \|D^s_-[v]\|_{\mathcal{M}(0,1)} + |I^{1-s}_-[v](1_-)| \;=\; \|D^s_-[v]\|_{\mathcal{M}(0,+\infty)}\,, \tag{3.3}$$

the symbol $\|\mu\|_{\mathcal{M}(E)}$ denotes the total variation of the real-valued measure μ in E.
A rational model for signal analysis must be invariant under mirror symmetry of the data. We underline that our model is orientation invariant, since the left and the right fractional derivatives are present, as it is clarified in the subsequent Remarks.

Remark 3.1. If u is a minimizer of $(\mathcal{P}_\mathcal{G})$ with datum g, then $\widetilde{u}$ is a minimizer of $(\mathcal{P}_\mathcal{G})$ with modified datum $\widetilde{g}$, by referring the notation $\widetilde{v}(x)=v(1-x)$.

Remark 3.2. If one drops the second summand (the one dependent on D^s_-) in the definition (3.1) of $\mathcal{G}$, then the evaluation of $\mathcal{G}(x^{s-1})$ would reduce to $\lambda\|x^{s-1}-g\|_{L^1}$, due to $D^s_+[x^{s-1}]=0$, whereas with present definition $\mathcal{G}(x^{s-1})=\lambda\|x^{s-1}-g\|_{L^1}+\|D^s_-[x^{s-1}]\|_T$ where $D^s_-[x^{s-1}]$ is nontrivial, since, by Lemma 8 in [34], $D^s_-[v]\equiv 0$ if and only if $v(x)=C(1-x)^{s-1}$. Actually, by formulas (A.1), (A.2) in [35] with $\alpha=s$ and $\beta=s-1$,

$$D^s_-[x^{s-1}] = -D_x I^{1-s}_-[x^{s-1}] = -D_x\left(\frac{1}{\Gamma(1-s)}\int_x^1 w^{-1}\,(1-w)^{-s}\,dw\right) \not\equiv 0\,.$$

Indeed $D^s_-[x^{s-1}]$ is analytic with a singularity at $x=0_+$ of the kind $(\Gamma(1-s))^{-1}(1-x)^{-s}/x$, therefore the measure $D^s_-[x^{s-1}]$ is not of bounded variation; hence $\forall s\in(0,1)$

$$x^{s-1}\in BV^s_+\setminus BV^s_-\,,\qquad (1-x)^{s-1}\in BV^s_-\setminus BV^s_+\,.$$

Therefore neither x^{s-1} nor $(1-x)^{s-1}$ belong to the space $BV^s(0,1)$; thus $\mathcal{G}(x^{s-1})=\mathcal{G}\big((1-x)^{s-1}\big)=+\infty$. This is a good property, since in signal processing one prefers to avoid unbounded outputs.
Summarizing: if one drops $\|D^s_+[u]\|$ when defining $\mathcal{G}$ then $(1-x)^{s-1}$ belongs to the domain; if one drops $\|D^s_-[u]\|$ then x^{s-1} belongs to the domain; whereas neither x^{s-1} nor $(1-x)^{s-1}$ belong to the domain of $\mathcal{G}$ with our definition.

Moreover, there are $v\in BV^s_+(0,1)\setminus BV^s_-(0,1)$ with nontrivial $D^s_+[v]$: for instance (see example 3.3. in [35]), consider

$$v(x) \;=\; H(x-1/2)\,|x-1/2|^{s-1}\,.$$

3.1. 1-dimensional SFV-L^1 model

Here, we demonstrate that problem $(\mathcal{P}_\mathcal{G})$ admits solutions.

Lemma 3.3. *For every sequence v_n bounded in $BV^s(0,1)$ such that $v_n\rightharpoonup v$ weakly in $L^1(0,1)$, we have*

$$\liminf \|D^s_+v_n\|_{T_+} \;\geq\; \|D^s_+v\|_{T_+}\,,\qquad \liminf \|D^s_-v_n\|_{T_-} \;\geq\; \|D^s_-v\|_{T_-}\,.$$

Proof. Sequence v_n is bounded in $L^p(0,1)$ $\forall p\in[1,1/(1-s))$, hence in $L^1(0,1)$ (by Theorem 2.6). Therefore we can argue as in the proof of Lemma 3.5 of [35]. □

Theorem 3.4. *If we assume that g belongs $L^1(0,1)$, then the functional $\mathcal{G}$ has a nonempty domain and is convex but not strictly convex; moreover the problem $(\mathcal{P}_\mathcal{G})$ achieves a finite minimum.*

Proof. Convexity of $\mathcal{G}$ is straightforward, because it is the sum of three convex terms.
The existence of minimizers follows by the direct methods of calculus of variations.
The functional $\mathcal{G}$ is bounded from below since $\mathcal{G}(v)\geq 0$ for every v.
Non-emptiness of domain follows by $0\leq\inf\mathcal{G}\leq\mathcal{G}(0)=\|g\|_{L^1(0,1)}<+\infty$.
Assume that v_n is a minimizing sequence. Then v_n is bounded in $L^p(0,1)$ for $1\leq p<1/(1-s)$, hence v_n is bounded in $L^1(0,1)$ and in

$BV^s(0,1)$ too.
Thus v_n converges weakly to some $\widetilde{v}$ in $L^p(0,1)$ for $1 \le p < 1/(1-s)$, possibly without relabeling and up to subsequences.
The sequences of derivatives $D^s_+ v_n$ and $D^s_- v_n$ are bounded in the space $\mathcal{M}$. Therefore by Theorem 2.6 there exists $\widetilde{v}$ in $BV^s(0,1)$, such that $D^s_+ v_n \to D^s_+ \widetilde{v}$, $D^s_- v_n \to D^s_- \widetilde{v}$ in the sense of weak* convergence of measures and $v_n \to \widetilde{v}$ in L^p weakly, if $1 \le p < 1/(1-s)$.
Summarizing, the existence of a minimizer follows by the lower semicontinuity of total variation with respect to the weak* convergence, as stated in Lemma 3.3, since $D^s_+[v_n]$ and $D^s_-[v_n]$ are bounded sequences of measures:

$$\|\widetilde{v} - g\|_{L^1(0,1)} = \|\widetilde{v} - g\|_{\mathcal{M}(0,1)} \le \liminf \|v_n - g\|_{\mathcal{M}(0,1)} = \liminf \|v_n - g\|_{L^1(0,1)} .$$

The fact that $\mathcal{G}$ is not strictly convex can be easily checked on constant functions: set $g \equiv 0$, then

$$\mathcal{G}(0) = 0, \qquad \mathcal{G}(c) = c\left(\lambda + \frac{2}{\Gamma(2-s)}\right), \qquad \forall\, c \in \mathbb{R}_+. \quad \square$$

Corollary 3.5 *(contrast equivariance). For any $s \in (0,1)$, $g \in L^1(0,1)$ and $\lambda \in \mathbb{R}_{++}$, the set $S(s,g,\lambda)$ of solutions to problem ($\mathcal{P}_\mathcal{G}$) is nonempty, convex and closed in the strong $L^1(0,1)$ norm, and, for any $\beta \in \mathbb{R}_{++}$,*

$$S(s, \beta g, \lambda) = \beta\, S(s,g,\lambda) . \qquad \text{[contrast equivariance]}$$

Proof. The claims are straightforward consequences of the Lemma 3.3, the Theorem 3.4 and the definition (3.1) which makes the functional $\mathcal{G}$ convex and 1-homogeneous. $\square$

Remark 3.6. Possible lack of uniqueness of the output is not a defect for a model in signal and image analysis. In this perspective, there are many successful nonconvex models in image analysis like Mumford-Shah and Blake-Zissermann functionals lacking uniqueness of minimizer, still they exhibit uniqueness as a generic property with respect to admissible data at least in the 1d setting: see [2,6]. This phenomenon aligns with the existence of unstable patterns. Each pattern represents a potential optimal segmentation outcome, but this optimality can change depending on variations in various parameters. These parameters include contrast threshold, luminance sensitivity, noise resistance, and edge detection settings.

Example 3.7. A more illustrative example about non strict convexity (and hence possibly non uniqueness of minimizers) is provided by choosing the datum g as the logistic function with normalized coefficient: in (3.1) we choose $g(x) = x(1-x)$, say a smooth function which vanishes at both end points (and extended with null value off $[0,1]$ when necessary), hence $D^s_\pm[g]$ has no singularities at all. Indeed, by $D^s_+[x^k] = x^{k-s}\frac{\Gamma(k+1)}{\Gamma(k+1-s)}$:

$$D^s_+[g] = \frac{x^{1-s}(2-s-2x)}{\Gamma(3-s)} \qquad D^s_-[g] = \frac{(1-x)^{1-s}(s-2x)}{\Gamma(3-s)},$$

$$\mathcal{G}(g) = \|D^s_+[g]\| + \|D^s_-[g]\| = \frac{(s-1) + 2^{-1+s}(2-s)^{2-s}}{\Gamma(4-s)} = \alpha \ge 1/6 > 0, \text{ if } 0<s<1,$$

$$\mathcal{G}(0) = \lambda \int_0^1 |g(x)|\, dx = \frac{1}{6}\lambda = \alpha, \text{ if } \lambda = 6\alpha .$$

$$\mathcal{G}(t\, g) = |t|\,\alpha + |1-t|\,\alpha = \alpha\Big(1 + 2\ \mathrm{dist}\,\big(t, [0,1]\big)\Big) \qquad \forall t \in \mathbb{R},$$

thus $\mathcal{G}$ is constant on the segment $\{\, t \mapsto t\, g : t \in [0,1] \,\}$ and $\mathcal{G}$ is affine linear on its complement in $\mathbb{R}$.

We introduce also the problems

$$\min \left\{ \mathcal{E}_+(v) :\ v \in \mathcal{M}_+ \right\}, \qquad (\mathcal{P}^+_\mathcal{E})$$

$$\min \left\{ \mathcal{E}_-(w) :\ w \in \mathcal{M}_- \right\}, \qquad (\mathcal{P}^-_\mathcal{E})$$

where $\mathcal{M}_+ := \{\mu \in \mathcal{M}(-\infty, 1) :\ \mathrm{spt}\,\mu \subset [0,1)\}$, $\mathcal{M}_- := \{\nu \in \mathcal{M}(0,+\infty) :\ \mathrm{spt}\,\nu \subset (0,1]\}$, the fractional integrals defined by (2.4), (2.5) have to be understood as the convolution of a measure with finite total variation and support in $[0,+\infty)$ (respectively $(-\infty,1]$) with the kernels $H(\pm x)(\Gamma(s))^{-1}|x|^{s-1}$ which belong to L^1_{loc} and have support respectively in $[0,+\infty)$ (respectively $(-\infty,0]$) (see [7], [29]), and

$$\mathcal{E}_+(v) := \lambda \left\| I^s_+[v] - g \right\|_{L^1} + \|v\|_{T_+} + \left\| D^s_- \left[I^s_+[v] \right] \right\|_{T_-}, \forall v \in \mathcal{M}_+,$$

$$\mathcal{E}_-(\mu) := \lambda \left\| I^s_-[\mu] - g \right\|_{L^1} + \|\mu\|_{T_-} + \left\| D^s_+ \left[I^s_-[\mu] \right] \right\|_{T_+}, \forall \mu \in \mathcal{M}_-,$$

Theorem 3.8. *If g belongs to $L^1(0,1)$ and s belongs to $(0,1)$, then the three problems $(\mathcal{P}_\mathcal{G})$, $(\mathcal{P}^+_\mathcal{E})$ and $(\mathcal{P}^-_\mathcal{E})$ are equivalent. Notably the problems $(\mathcal{P}^+_\mathcal{E})$ and $(\mathcal{P}^-_\mathcal{E})$ achieve a finite minimum.*

Proof. We claim that the two changes of variable, v replaces u or μ replaces u, defined respectively by $u = I^s_+[v]$ and $u = I^s_-[w]$, are bijective (respectively from $\operatorname{dom}\mathcal{E}_+$ and $\operatorname{dom}\mathcal{E}_-$ into $BV^s \cap L^1$). We verify that both variable changes are bijective.
If v belongs to $\operatorname{dom}\mathcal{E}_+ := \{v \in \mathcal{M}^+ : I^s_+[v] \in L^1(0,1)\}$ then there exists a unique $u = I^s_+[v] \in L^2(0,1)$, such that $I^{1-s}_+[u](x) = I^{1-s}_+[I^s_+[v]](x) = \int_0^x v \in BV$ since it is the primitive of a bounded measure, thus $u \in BV^s_+ \cap L^1$; moreover $D^s_-[u] = D^s_-\left[I^s_+[v]\right]$, hence $u = I^s_+[v] \in BV^s_-$, by the finiteness of the functional. Hence $u \in \operatorname{dom}\mathcal{G}$.
Exactly in the same way, one can verify that for every $\mu \in \operatorname{dom}\mathcal{E}_- := \{\mu \in \mathcal{M}^- : I^s_-[\mu] \in L^1(0,1)\}$ there exists a uniquely defined $u = I^s_-[\mu] \in \operatorname{dom}\mathcal{G}$.
Vice versa, for all $u \in \operatorname{dom}\mathcal{G} = BV^s \cap L^1 = \{u \in L^1(0,1) : I^{1-s}_+[u], I^{1-s}_-[u] \in BV(0,1)\}$, due to Propositions 3 and Corollary 2 in [34] we can solve these two equations in the distributional framework

$$u = I^s_+[v], \qquad u = I^s_-[\mu],$$

namely the forward Abel integral equations in the unknown v and the backward Abel integral equations in the unknown μ. We find a unique Laplace transformable solution μ and unique solution v among Laplace transformable distribution computed in the variable $1-x$, which are explicitly provided by:

$$\mu(x) = D^s_+[u](x) + I^{1-s}_+[u](0_+)\,\delta(x)$$

$$v(x) = D^s_-[u](x) + I^{1-s}_-[u](1_-)\,\delta(x-1)$$

The equivalence follows by plain substitution: set $u = I^s_+[\mu] = I^s_-[v]$, take into account the identities $D^s_+[I^s_+[u]] = u$, $D^s_-[I^s_-[u]] = u$ (see (117), (121) in [34]), whence

$$\mathcal{G}(u) = \mathcal{E}_+(\mu) = \mathcal{E}_-(v)\,.$$

Eventually, by equivalence with problem $(\mathcal{P}_\mathcal{G})$

$$I^s_+[\mu] \in \operatorname{argmin}\mathcal{G} \qquad \forall \mu \in \operatorname{argmin}\mathcal{E}_+$$

$$I^s_-[v] \in \operatorname{argmin}\mathcal{G} \qquad \forall v \in \operatorname{argmin}\mathcal{E}_-$$

$$D^s_+[u] + I^{1-s}_+[u](0_+)\delta(x) \text{ belongs to } \operatorname{argmin}\mathcal{E}_+ \text{ for every } u \in \operatorname{argmin}\mathcal{G},$$

$$D^s_-[u] + I^{1-s}_-[u](1_-)\delta(x-1) \text{ belongs to } \operatorname{argmin}\mathcal{E}_- \text{ for every } u \in \operatorname{argmin}\mathcal{G},$$

and by bijectivity of variable changes we get the existence of minimizers for both problems $(\mathcal{P}^+_\mathcal{E})$ and $(\mathcal{P}^-_\mathcal{E})$. □

3.2. Optimality conditions

We refer to the representations (as provided by Lemma 3.8 in [35]) of the adjoint operators for fractional integrals and fractional derivatives aiming to show some necessary conditions for the candidate minimizers of the problem $(\mathcal{P}_\mathcal{G})$.

Lemma 3.9. *Any minimizer w of problem $(\mathcal{P}_\mathcal{G})$ fulfills*

$$0 \in \lambda\,\partial(\|\cdot\|_{L^1})(w-g) + (D^s_+)^*\left[\partial T_+(D^s_+[w])\right] + (D^s_-)^*\left[\partial T_-(D^s_-[w])\right] \text{ in } \mathcal{D}'(0,1), \tag{3.4}$$

where ∂J is the subdifferential of J and $\partial T_\pm$ denote the selections fulfilling local integrability of $D^s_+[\partial T_+[w]]$ and $D^s_-[\partial T_-[w]]$.

Proof. The subdifferential of $\mathcal{G}$ is a (possibly multivalued) maximal monotone operator with values in the dual space of BV^s ([10]). The null element of dual space belongs to this subdifferential when evaluated at a minimizer of $\mathcal{G}$.
For every minimizer w we can perform smooth variations $w + \varepsilon\psi$ with smooth ψ and ε in $\mathbb{R}$, thus obtaining $0 \in \partial\mathcal{G}(w)$ and

$$\langle\, \partial\mathcal{G}(w), \psi \,\rangle = \lambda\,\partial(\|\cdot\|_{L^1})(w-g) + \langle\, \partial T_+\left[D^s_+[w]\right], D^s_+[\psi] \,\rangle + \langle\, \partial T_-\left[D^s_-[w]\right], D^s_-[\psi] \,\rangle$$

thus (3.4) is achieved. □

Remark 3.10. If $\mathcal{G}(w) < +\infty$ and, either $D^s_+[w] \equiv 0$ or $D^s_-[w] \equiv 0$, then $w \equiv 0$.
Indeed, if $D^s_+[w] \equiv 0$ then $w = Cx^{s-1}$ and (by Remark 3.2) $D^s_-[x^{s-1}] \notin \mathcal{M}$, hence $\mathcal{G}(Cx^{s-1}) < +\infty$ entails $C = 0$, $w \equiv 0$. Likewise, $\mathcal{G}(w) < +\infty$ and $D^s_-[w] \equiv 0$ entail $w \equiv 0$.

4. Relations between Riemann-Liouville and Grünwald-Letnikov fractional derivatives

In order to perform numerical experiments with SFV-L^1 model we exploited the truncated Grünwald-Letnikov scheme to evaluate one sided fractional derivatives.
The approach suggested independently by Grünwald 1867 [26], and Letnikov 1868 [36], is based on the limits of the difference quotients, similar to the classical definition of the derivative for $m \in \mathbb{N}$, given $u \in C^m[a,b]$,

$$\frac{d^m u(x)}{dx^m} = \lim_{h\to 0_+} \frac{\Delta_h^m u(x)}{h^m}, \qquad a < x < b,$$

where, by generalizing the first-order difference $u(x-h)-u(x)$, $\Delta_h^m u(x)$ denotes the mth order difference

$$(\Delta_h^m u)(x) = \sum_{k=0}^{m} (-1)^k \binom{m}{k} u(x-kh), \tag{4.1}$$

with h the uniform space step. Since $\binom{m}{k} = 0$ if $m \in \mathbb{N}$ and $m < k$, then the expression (4.1) is equivalent to

$$(\Delta_h^m u)(x) = \sum_{k=0}^{+\infty} (-1)^k \binom{m}{k} u(x-kh). \tag{4.2}$$

The series (4.2) is uniformly convergent for any bounded function u if $m > 0$. Then the definition of the Grünwald-Letnikov fractional derivatives follows by generalizing to the case of an arbitrary (not necessary integer) order m.

Definition 4.1. Grünwald-Letnikov fractional derivative
Assume u is an analytic function in a complex neighborhood of the real line and s is a real number fulfilling $s > 0$. Then the direct and reverse Grünwald-Letnikov derivative of order s of u at $x \in \mathbb{R}$ (respectively $\mathfrak{D}_+^s$ and $\mathfrak{D}_-^s$) are defined by:

$$\mathfrak{D}_+^s[u](x) = \lim_{h\to 0_+} \frac{1}{h^s} \sum_{k=0}^{+\infty} (-1)^k \binom{s}{k} u(x-kh), \tag{4.3}$$

$$\mathfrak{D}_-^s[u](x) = \lim_{h\to 0_+} \frac{1}{h^s} \sum_{k=0}^{+\infty} (-1)^k \binom{s}{k} u(x+kh). \tag{4.4}$$

It is well known ([41], [48]) that if u is an analytic function on $\mathbb{C}$ off the negative real line then $\mathfrak{D}_+^s[u](x)$ is equal to the generalized Cauchy fractional derivative ${}_C D[u](x)$ as given by

$${}_C D_+^s[u](z) = \frac{\Gamma(s+1)}{2\pi i} \int_\gamma \frac{u(w)}{(w-z)^{s+1}}\, dw \tag{4.5}$$

where we assume that the branch cut line is inside the above referred analyticity region, and γ is a U shaped contour encircling the branch cut line (negative real axis).
Expression (4.5) agrees with the usual derivative definition when s is a positive integer.
Both (4.3) and (4.4) are absolutely convergent if u is continuous and bounded on the real line. When dealing with a function u defined on a bounded interval of $\mathbb{R}$, we can apply to u the definitions (4.3) and (4.4), by considering the periodic extension of u.

Definition 4.2. Let $u \in L^p(0,1)$ and $s \in (0,1)$.
Then the **left Marchaud derivative** of u at $x \in (0,1]$ is defined by

$$\mathbb{D}_+^s[u] = \lim_{\varepsilon\to 0} \mathbb{D}_{+,\varepsilon}^s[u]$$

in L^p with respect to the strong topology with

$$\mathbb{D}_{+,\varepsilon}^s[u](x) = \frac{u(x)}{\Gamma(1-s)(x-a)^s} + \frac{s}{\Gamma(1-s)}\, \psi_\varepsilon(x)$$

and

$$\psi_\varepsilon(x) = \begin{cases} \displaystyle\int_0^{x-\varepsilon} \frac{u(x)-u(t)}{(x-t)^{1+s}}\, dt & \text{if } x \ge \varepsilon, \\ \displaystyle\int_0^{x-\varepsilon} \frac{u(x)}{(x-t)^{1+s}}\, dt & \text{if } 0 \le x \le \varepsilon. \end{cases}$$

Here the definition of ψ_ε for $0 \le x \le \varepsilon$ is obtained by extending the function u with zero value outside the interval $[0,1]$. The passage to the limit depends on the function space we are working with. We remark that such a derivative is not defined at $x = 0$ and that a necessary condition for the existence of the derivative is $u(0) = 0$

The right derivative can be defined analogously by using the integral between x and b. In the following we state the main results about Marchaud differentiation for the left-side derivative, but similar results can be obtained for the right-side one.

If u is a C^1-function, the Marchaud and Riemann-Liouville derivatives coincide for every $s \in (0,1)$ (see Theorems 13.1, 13.2 in [48]):

$$\forall\, u \in C^1([0,1]), \qquad D^s_+[u](x) = \mathbb{D}^s_+[u](x) \quad \forall\, x \in (0,1]\,,$$

actually,

$$\forall\, u \in C^{0,s+\alpha}\big([0,1]\big),\ 0 < \alpha < 1 - s, \qquad D^s_+[u](x) = \mathbb{D}^s_+[u](x) \quad \text{for a.e. } x \in (0,1]\,.$$

Moreover the Grünwald-Letnikov and Marchaud derivatives coincide for periodic functions (see Section 20 in [48]: Th.20.2. and also [25]):

$$\begin{aligned} &\forall\, u \in L^p(0,1) \text{ (or } u \in L^p(\mathbb{R})), \quad \mathbb{D}^s_{a+}[u] \in L^p \ \text{ iff } \ \mathfrak{D}^s_+[u] \in L^p \text{ too,} \\ &\text{moreover,} \qquad \mathbb{D}^s_+[u](x) = \mathfrak{D}^s_+[u](x) \qquad \forall u \in W^{s,1}(0,1)\,, \end{aligned} \tag{4.6}$$

where $W^{s,1}$ denotes the fractional Sobolev space (see Definition 2.3).

These are useful tools in order to deal with the fractional derivatives because the Marchaud and Grünwald-Letnikov derivatives are easier to handle than the Riemann-Liouville ones.

In signal/image processing the most frequently used fractional derivatives are the Grünwald-Letnikov (see e.g. [37]).

The fractional derivatives are nonlocal operators for any non-integer s: indeed the value of the left-sided (right-sided) fractional derivative at a point x depends on the function values at all the points to the left (right) of the point x. The reduction of the computational efforts resorts to the fading memory property of the fractional derivatives that allows to restrict the integration interval using the "short-memory" principle [43]. This technique truncates the approximation sum in (4.3)-(4.4) to avoid high computational cost and memory requirements.

Definition 4.3. The **truncated Grünwald-Letnikov scheme** of fractional order s is defined for a function $u \in C^0[0,1]$, by

$${}_{\mathrm{GL}}\Delta^s_\pm[u](x) = \frac{1}{h^s}\sum_{k=0}^{K}(-1)^k \binom{s}{k} u(x \mp kh), \tag{4.7}$$

where ${}_{\mathrm{GL}}\Delta^s_+$ denotes the left-sided and ${}_{\mathrm{GL}}\Delta^s_-$ the right-sided GL derivative; K is a positive integer expressing the unitary length of the support with respect to the scale $x>0$: $K = \lceil x/h \rceil$ for left-sided, $K = \lceil (1-x)/h \rceil$ for right-sided; $\lceil t \rceil$ is the ceiling of t.

Note that (4.7) is coherent, actually coincident with the series (4.3) if the RL fractional derivatives are defined by (2.2)-(2.5) via convolution involving the trivial extension of u outside $(0,1)$.

Therefore, we will use in the following the approximation $\mathfrak{D}^s_\pm[u](x) \approx {}_{\mathrm{GL}}\Delta^s_\pm[u](x)$, arising from the Grünwald–Letnikov Definition 4.1.

5. Fractional difference approach of the proposed model

5.1. Discretization of the domain

First, without loss of generality, we introduce a uniform discretization of the unitary 1d domain $[0,1] \subset \mathbb{R}$ considered in the continuous setting. In particular, we define the 1d grid of n points:

$$\big\{\, x_i = i\,h\,,\ i = 0, \dots, n-1\,,\ h = 1/(n-1)\,\big\}\,. \tag{5.1}$$

We indicate by $\boldsymbol{u} := (u_0, \dots, u_i, \dots, u_{n-1})^{\mathrm{T}} \in \mathbb{R}^n$ the (column) vector containing the values that function u assumes at all the grid points.

5.2. Approximation of Riemann-Liouville fractional derivatives

The standard shifted left and right Grünwald difference operators ${}_{\mathrm{GL}}\Delta^s_+$, ${}_{\mathrm{GL}}\Delta^s_-$ approximate the left and right Riemann-Liouville fractional derivatives D^s_+ and D^s_- uniformly with first order accuracy; in formula,

$${}^{p}_{\mathrm{GL}}\Delta^s_+[u](x_i) \;=\; \frac{1}{h^s}\sum_{k=0}^{K}\omega^s_k\, u_{i+p-k} = D^s_+[u](x_i) + O(h), \tag{5.2}$$

$$ {}^{p}_{\mathrm{GL}}\Delta^{s}_{-}[u](x_i) \;=\; \frac{1}{h^s}\sum_{k=0}^{K}\omega_k^s\, u_{i-p+k} = D^s_{-}[u](x_i) + O(h), \tag{5.3} $$

where the coefficients ω_k^s are defined as follows

$$ \omega_k^s \;=\; (-1)^k\binom{s}{k} = (-1)^k\frac{\Gamma(s+1)}{\Gamma(k+1)\Gamma(s-k+1)}\;, \quad k\in\mathbb{N}. \tag{5.4} $$

The generalized binomial coefficients $\binom{s}{k}$, defined in (5.4) in terms of the Gamma function, can be computed by the following recurrence relationships

$$ \omega_0^s = 1; \quad \omega_k^s = \omega_{k-1}^s\cdot\left(1-\frac{s+1}{k}\right), \quad k = 1,2,\dots. $$

In [50] the authors introduced second (and higher) order approximations for the Riemann-Liouville fractional derivatives based on the shifted Grünwald operator. In particular, the left and right weighted and shifted Grünwald difference operators are defined as follows

$$ {}^{p,q}_{\mathrm{GL2}}\Delta^{s}_{+}[u](x) = \frac{s-2q}{2(p-q)}\,{}^{p}_{\mathrm{GL}}\Delta^{s}_{+}[u](x) + \frac{2p-s}{2(p-q)}\,{}^{q}_{\mathrm{GL}}\Delta^{s}_{+}[u](x) = D^s_{+}[u](x) + O(h^2), \tag{5.5} $$

$$ {}^{p,q}_{\mathrm{GL2}}\Delta^{s}_{-}[u](x) = \frac{s-2q}{2(p-q)}\,{}^{p}_{\mathrm{GL}}\Delta^{s}_{-}[u](x) + \frac{2p-s}{2(p-q)}\,{}^{q}_{\mathrm{GL}}\Delta^{s}_{-}[u](x) = D^s_{-}[u](x) + O(h^2), \tag{5.6} $$

where p, q are integers and $p \neq q$.

Considering the uniform domain discretization we can rewrite formulas (5.5) and (5.6) in a more compact form

$$ {}^{p,q}_{\mathrm{GL2}}\Delta^{s}_{+}[u](x_i) \;=\; \frac{1}{h^s}\sum_{k=0}^{K} w_k^s\, u_{i+\max(p,q)-k} + O(h^2), \tag{5.7} $$

$$ {}^{p,q}_{\mathrm{GL2}}\Delta^{s}_{-}[u](x_i) \;=\; \frac{1}{h^s}\sum_{k=0}^{K} w_k^s\, u_{i-\max(p,q)+k} + O(h^2). \tag{5.8} $$

If (p, q) in (5.5)-(5.6) is $(1, -1)$, then

$$ w_0^s = \frac{2+s}{4}\omega_0^s\;,\; w_1^s = \frac{2+s}{4}\omega_1^s\;,\; w_k^s = \frac{2+s}{4}\omega_k^s + \frac{2-s}{4}\omega_{k-2}^s, \quad k\geq 2. $$

5.3. Discretization of the norms

In order to discretize the two norms appearing in the proposed 1d model (3.1) related to the symmetrized regularization term, we note that when $I^{1-s}[u]$ is an absolutely continuous function vanishing at $x=0$ and $x=1$, then the two noise-filtering terms read as Lebesgue integrals

$$ \|D^s_{+}[u]\|_{T_+} \;=\; \int_0^1 \left|D^s_{+}[u](x)\right| dx\,, \qquad \|D^s_{-}[u]\|_{T_-} \;=\; \int_0^1 \left|D^s_{-}[u](x)\right| dx\,, $$

and, in such case, we can consider any quadrature rule using equally spaced quadrature nodes. In particular, to the aim of achieving a good accuracy-efficiency tradeoff, in the following we consider the composite Newton-Cotes quadrature formulas of degree 0 (midpoint rule) and 2 (Simpson's rule). Upon suitable conditions on the integrand function, the two rules exhibit orders of accuracy equal to 2 and 4 - that is, the quadrature error is $O(h^2)$ and $O(h^4)$, with h the mesh step size, respectively.

In the following example, we support experimentally our subsequent choices for the discretizations of the fractional derivatives as well as of the definite integrals.

Example. We consider the function

$$ u(x) = x^2\,(1-x)^2 = x^4 - 2x^3 + x^2\,. \tag{5.9} $$

It can be easily proved that the left and right Riemann-Liouville fractional derivatives of order $s\in(0,1)$ of u are given by

$$ \begin{aligned} D^s_{+}[u](x) \;&=\; D^s_{+}[x^4](x) - 2D^s_{+}[x^3](x) + D^s_{+}[x^2](x) \\ &=\; \frac{\Gamma(5)}{\Gamma(5-s)}\,x^{4-s} - 2\frac{\Gamma(4)}{\Gamma(4-s)}\,x^{3-s} + \frac{\Gamma(3)}{\Gamma(3-s)}\,x^{2-s}\,, \end{aligned} \tag{5.10} $$

$$ D^s_{-}[u](x) \;=\; -D^s_{+}[u](1-x). \tag{5.11} $$

Moreover, for the specific case $s = 0.5$, it can be proved that the fractional derivative $D^{0.5}_{+}[u](x)$ has a unique zero x_0 in the interval $(0, 1)$ given by

$$x_0 = \frac{7}{8}\left(1 - \frac{1}{\sqrt{21}}\right) = \frac{1}{8}\left(7 - \sqrt{\frac{7}{3}}\right),$$

and we have that

$$D_+^{0.5}[u](x) > 0 \text{ for } x \in [0, x_0), \quad D_+^{0.5}[u](x) < 0 \text{ for } x \in (x_0, 1].$$

In Fig. 1 - first row - we show the graphs of $u(x)$ and $D_+^{0.5}[u](x)$, as well as the zero x_0, marked by a red dot.

We first compare experimentally the accuracy of the first-order left GL formula in (5.2) and second-order left GL2 formula in (5.7) in approximating the left fractional derivative with order $s = 0.5$ of the function $u(x)$ in (5.9). The accuracy is measured by the relative error of approximation,

$$E(x,h) := \frac{\left|D_+^s[u](x) - \Delta_+^s[u](x)\right|}{\left|D_+^s[u](x)\right|}, \tag{5.12}$$

where, we remark, we made the dependence of the relative error on the point of differentiation x as well as on the step-size h of the uniform domain mesh explicit.

The errors $E(x,h)$ in (5.12) are reported in Fig. 1 for $\Delta_+^{0.5}[u](x)$ being the left GL or GL2 (1st and 2nd order) formulas. The two graphs reported in the second row of Fig. 1 consider a fixed point of differentiation $x = 0.2$. In the left panel we show the relative error of approximation $E(x = 0.2, h)$ as a function of the step-size h using all the $K = \lfloor x/h \rfloor$ terms in the GL and GL2 formulas, whereas in the right panel the error $E(x = 0.2, h = 10^{-3})$ is plotted as a function of a (reduced) varying number K of terms. In the third row of Fig. 1, on the left, in order to analyze the approximation error over the entire domain of u, we show $E(x, h = 10^{-3})$. These first experiments confirm the theoretical expectations and motivate us to use the GL2 approximation of the fractional derivatives. In particular, we will use the GL2 discretization with $p = 1$, $q = -1$.

In the second part of this experiment we evaluate the accuracy of approximation of the overall $\mathrm{FV}_+^{0.5}[u]$ regularization term achieved by using the composite midpoint and Simpson 1/3 Newton-Cotes quadrature rules. The analytical evaluation of $\mathrm{FV}_+^{0.5}[u]$ reads

$$\begin{aligned}
\|D_+^{0.5}[u]\|_{T_+} &= \int_0^1 \left|D_+^{0.5}[u](x)\right| dx = \int_0^{x_0} D_+^{0.5}[u](x)dx \; - \int_{x_0}^1 D_+^{0.5}[u](x)dx \\
&= \left[\frac{\Gamma(5)}{\Gamma(5.5)}x^{4.5} - 2\frac{\Gamma(4)}{\Gamma(4.5)}x^{3.5} + \frac{\Gamma(3)}{\Gamma(3.5)}x^{2.5}\right]_0^{x_0} \\
&\quad - \left[\frac{\Gamma(5)}{\Gamma(5.5)}x^{4.5} - 2\frac{\Gamma(4)}{\Gamma(4.5)}x^{3.5} + \frac{\Gamma(3)}{\Gamma(3.5)}x^{2.5}\right]_{x_0}^1 \\
&\approx 0.056983968818256.
\end{aligned} \tag{5.13}$$

We remark that the actual accuracy of the $\mathrm{FV}_+^{0.5}[u]$ regularizer is affected by both the quadrature error and the fractional derivative approximations, and it can be measured by the relative error

$$E_{\mathrm{QUAD}}^{\mathrm{DER}} := \frac{|\mathrm{FV}_+^{0.5}[u] - I_{\mathrm{QUAD}}^{\mathrm{DER}}[u]|}{|\mathrm{FV}_+^{0.5}[u]|}, \quad \mathrm{DER} \in \{\mathrm{GL}, \mathrm{GL2}\}, \; \mathrm{QUAD} \in \{\mathrm{MID}, \mathrm{SIM}\}.$$

In the right panel of the last row of Fig. 1 we show the relative error of approximation $E_{\mathrm{QUAD}}^{\mathrm{DER}}$ for the four combinations considered as a function of the total number n of equally spaced nodes in the considered mesh, clearly given by $n = 1/h$ with h the mesh step-size. Moreover, in Table 1 we report the actual approximation errors are reported for a set of different values of n ranging from $n = 41$ to $n = 1001$.

It can be observed that the theoretical linear and quadratic trends reported in Fig. 1 (dashed lines) reveal the actual relationship between the errors of the methods, and highlights that the best performing numerical solution for the approximation of the FV_+^s regularizer is to apply the $O(h^2)$ composite midpoint Newton-Cotes rule together with the $O(h^2)$ GL2 fractional derivative approximation formula.

5.4. Model discretization

To discretize the model, first we introduce the two matrices

$$\mathbf{D}_+^s, \mathbf{D}_-^s \in \mathbb{R}^{n \times n} \tag{5.14}$$

which, under right multiplication times the column vector $\boldsymbol{u} = (u_0, \ldots, u_{n-1})^{\mathrm{T}} \in \mathbb{R}^n$ containing the values assumed by the function $u : [0,1] \to \mathbb{R}$ at all the 1d grid points in (5.1), compute the two vectors of left and right weighted and shifted Grünwald differences -

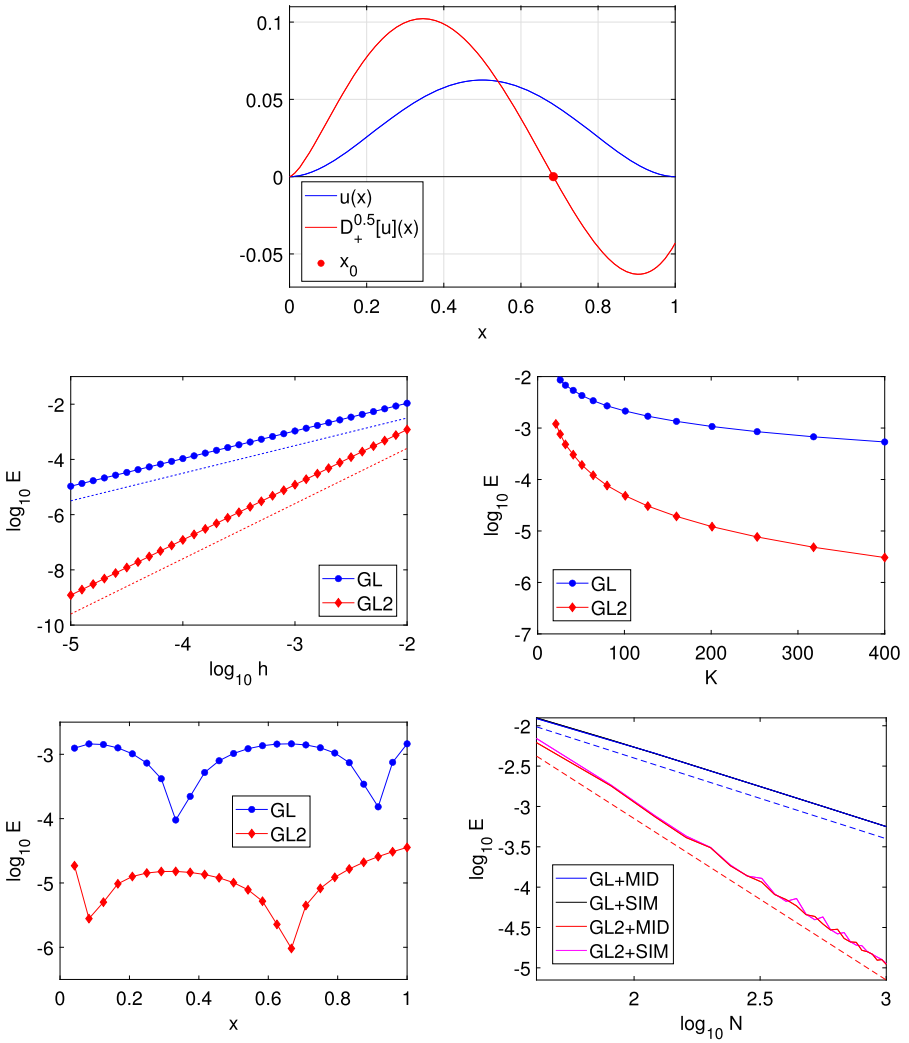

Fig. 1. First row: function $u(x) = x^2(1-x)^2$ (blue colored), its left Riemann-Liouville fractional derivative (red colored) and its zero in $(0,1)$ (red dot). Second row: approximation error $E(x=0.2,h)$ of $D_+^{0.5}[u](0.2)$ with left-side GL and GL2 formulas. From left to right: $E(x=0.2,h)$ for varying h values and for increasing K values. Third row, from left to right: derivative approximation error $E(x,h=10^{-3})$ for varying x, and quadrature approximation error $E_{\text{QUAD}}^{\text{DER}}$ for the FV_+^s regularizer with left-side GL and GL2 formulas and composite midpoint and Simpson 1/3 quadrature rules.

Table 1
Numerical approximation errors $E_{\text{QUAD}}^{\text{DER}}$ (%) for a set of n nodes, for the different fractional derivative formulas (GL, GL2) and quadrature rules (MID, SIM).

n	41	71	101	151	201	301	401	501	1001
$E_{\text{MID}}^{\text{GL}}$	1.2298	0.7560	0.5338	0.3598	0.2759	0.1858	0.1390	0.1122	0.0563
$E_{\text{SIM}}^{\text{GL}}$	1.2527	0.7234	0.5466	0.3675	0.2767	0.1863	0.1388	0.1119	0.0563
$E_{\text{MID}}^{\text{GL2}}$	0.6182	0.2355	0.1034	0.0491	0.0308	0.0117	0.0070	0.0045	0.0011
$E_{\text{SIM}}^{\text{GL2}}$	0.6963	0.2233	0.1063	0.0499	0.0311	0.0136	0.0067	0.0045	0.0011

see the definitions in (5.7)-(5.8) - approximating the fractional derivatives of u at those points. In particular, it is easy to verify that the r-th rows of matrices $\mathbf{D}_+^s$ and $\mathbf{D}_-^s$ read

$$\left(\mathbf{D}_+^s\right)_r = \left(w_r^s, \dots, w_{\max(0,r-(n-1))}^s, 0_{n-r-1}\right), \tag{5.15}$$

$$\left(\mathbf{D}_-^s\right)_r = \left(0_{r-2}, w_{\max(0,2-r)}^s, \dots, w_{n-r+1}^s\right), \tag{5.16}$$

for $r = 1, \cdots, n$. Hence, $\mathbf{D}_+^s$ and $\mathbf{D}_-^s$ are lower and upper Hessemberg matrices, respectively, and $\mathbf{D}_+^s = (\mathbf{D}_-^s)^T$.

If Dirichlet homogeneous boundary conditions are considered, then the two matrices in (5.14) are Toeplitz. If, instead, periodic boundary conditions are adopted, matrices are circulant.

Suitable truncation strategies of the sums in (5.2)-(5.3) and, hence, in (5.7)-(5.8) have been proposed, e.g., in [37].

By exploiting previous definitions, the discretized model reads

$$\widehat{\boldsymbol{u}}(s,\lambda) \in \operatorname{argmin}_{\boldsymbol{u}\in\mathbb{R}^n} \left\{ G(\boldsymbol{u};s,\lambda) := \mathrm{SFV}^s(\boldsymbol{u}) + \lambda \left\|\boldsymbol{u}-\boldsymbol{g}\right\|_1 \right\}, \tag{5.17}$$

with the SFV^s regularizer defined by

$$\mathrm{SFV}^s(\boldsymbol{u}) = \left\|\mathbf{D}^s_- \boldsymbol{u}\right\|_1 + \left\|\mathbf{D}^s_+ \boldsymbol{u}\right\|_1, \tag{5.18}$$

where we made explicit the dependency of the solution $\widehat{\boldsymbol{u}}$ on the parameter pair (s,λ).

Referring to (3.2), (3.3), we emphasize that $\left\|\mathbf{D}^s_\pm \mathbf{u}\right\|_1$ is an approximation of $\left\|D^s_\pm u\right\|_{T_\pm}$.

Starting from definition (5.14), and introducing the matrix

$$\mathbf{D}^s := \begin{pmatrix} \mathbf{D}^s_+ \\ \mathbf{D}^s_- \end{pmatrix} \in \mathbb{R}^{2n\times n}, \tag{5.19}$$

the SFV^s regularizer in (5.18) can be compactly rewritten as

$$\mathrm{SFV}^s(\boldsymbol{u}) = \left\|\mathbf{D}^s \boldsymbol{u}\right\|_1. \tag{5.20}$$

The following result provides the main properties of cost function G which lead to the existence of solutions of the minimization problem in (5.17).

Proposition 5.1. *For any $s,\lambda\in\mathbb{R}_{++}$ and any data $\boldsymbol{g}\in\mathbb{R}^n$, the cost function G defined in (5.17) is proper, continuous, convex and coercive in $\boldsymbol{u}$, hence the minimization problem in (5.17) admits a compact convex set of solutions.*

Proof. The function G in (5.17) is proper, continuous, convex and coercive as it is given by the sum of two functions which, for any $s,\lambda\in\mathbb{R}_{++}$, $g\in\mathbb{R}^n$, are both clearly proper, continuous, convex and bounded below by zero, with the second being coercive. It is then a classical result of convex analysis that a function having the properties of G admits a compact and convex set of global minimizers. □

6. Numerical solution by ADMM

For the solution of the finite-dimensional minimization problem (5.17) we use an efficient iterative algorithm based on the Alternating Direction Method of Multipliers (ADMM). After introducing the auxiliary variable $\boldsymbol{y}$ defined by

$$\boldsymbol{y} = \begin{pmatrix} \boldsymbol{y}_1 \\ \boldsymbol{y}_2 \end{pmatrix} = \begin{pmatrix} \mathbf{D}^s \boldsymbol{u} \\ \boldsymbol{u} \end{pmatrix} \in \mathbb{R}^{3n},$$

it is easy to verify that our discrete model (5.17) with the SFV^s regularization term defined in (5.19)-(5.20) can be equivalently reformulated as a standard two-blocks (additively) separable minimization problem with linear constraints,

$$\left\{\widehat{\boldsymbol{u}}(s,\lambda), \widehat{\boldsymbol{y}}(s,\lambda)\right\} \in \operatorname{argmin}_{\boldsymbol{u},\boldsymbol{y}} \left\{ U(\boldsymbol{u}) + Y(\boldsymbol{y};\lambda) \right\} \text{ subject to } \mathbf{U}^s\boldsymbol{u} + \mathbf{Y}\boldsymbol{y} = \mathbf{0}, \tag{6.1}$$

with the two cost functions U and Y defined by

$$U(\boldsymbol{u}) \equiv 0, \qquad Y(\boldsymbol{y};\lambda) = \left\|\boldsymbol{y}_1\right\|_1 + \lambda \left\|\boldsymbol{y}_2 - \boldsymbol{g}\right\|_1, \tag{6.2}$$

and with matrices $\mathbf{U}^s$, $\mathbf{Y}$ given by

$$\mathbf{U}^s = \begin{pmatrix} \mathbf{D}^s \\ \mathbf{I}_n \end{pmatrix} \in \mathbb{R}^{3n\times n}, \quad \mathbf{Y} = -\mathbf{I}_{3n}. \tag{6.3}$$

The Lagrangian function $\mathcal{L}$ and augmented Lagrangian function $\mathcal{L}_\beta$ associated with problem (6.1) read

$$\mathcal{L}(\boldsymbol{u},\boldsymbol{y},\boldsymbol{\rho};s,\lambda) = U(\boldsymbol{u}) + Y(\boldsymbol{y};\lambda) + \boldsymbol{\rho}^{\mathrm{T}}\left(\mathbf{U}^s\boldsymbol{u} + \mathbf{Y}\boldsymbol{y}\right), \tag{6.4}$$

$$\mathcal{L}_\beta(\boldsymbol{u},\boldsymbol{y},\boldsymbol{\rho};s,\lambda) = \mathcal{L}(\boldsymbol{u},\boldsymbol{y},\boldsymbol{\rho};\lambda) + \frac{\beta}{2}\left\|\mathbf{U}^s\boldsymbol{u} + \mathbf{Y}\boldsymbol{y}\right\|_2^2, \tag{6.5}$$

where $\beta\in\mathbb{R}_{++}$ is a penalty parameter and $\boldsymbol{\rho}\in\mathbb{R}^{3n}$ is the vector of Lagrange multipliers associated to the system of linear constraints in (6.1).

Solving problem (6.1) amounts to seek the saddle point(s) of the augmented Lagrangian function $\mathcal{L}_\beta$ in (6.5); in formula,

$$\{\widehat{\boldsymbol{u}}(s,\lambda), \widehat{\boldsymbol{y}}(s,\lambda), \widehat{\boldsymbol{\rho}}(s,\lambda)\} \in \arg\min_{\boldsymbol{u},\boldsymbol{y}} \max_{\boldsymbol{\rho}} \mathcal{L}_\beta(\boldsymbol{u},\boldsymbol{y},\boldsymbol{\rho};s,\lambda). \tag{6.6}$$

The solution(s) of the saddle-point problem (6.6) can be computed as the limit point(s) of the standard two-blocks ADMM algorithm [8]. Upon suitable initialization, and for any $k \geq 0$, the k-th iteration of the algorithm reads as follows:

$$\begin{aligned}
\boldsymbol{u}^{(k+1)} &= \operatorname{argmin}_{\boldsymbol{u}} \mathcal{L}_\beta\left(\boldsymbol{u}, \boldsymbol{y}^{(k)}, \boldsymbol{\rho}^{(k)}; s, \lambda\right) && (6.7)\\
&= \operatorname{argmin}_{\boldsymbol{u}} \left\{ U(\boldsymbol{u}) + \frac{\beta}{2} \left\| \mathbf{U}^s \boldsymbol{u} + \mathbf{Y}\boldsymbol{y}^{(k)} + \frac{1}{\beta}\boldsymbol{\rho}^{(k)} \right\|_2^2 \right\} && (6.8)\\
&= \operatorname{argmin}_{\boldsymbol{u}} \frac{1}{2} \left\| \mathbf{U}^s \boldsymbol{u} - \boldsymbol{q}^{(k)} \right\|_2^2, \quad \boldsymbol{q}^{(k)} = \boldsymbol{y}^{(k)} - \frac{1}{\beta}\boldsymbol{\rho}^{(k)}, && (6.9)
\end{aligned}$$

$$\begin{aligned}
\boldsymbol{y}^{(k+1)} &= \operatorname{argmin}_{\boldsymbol{y}} \mathcal{L}_\beta\left(\boldsymbol{u}^{(k+1)}, \boldsymbol{y}, \boldsymbol{\rho}^{(k)}; s, \lambda\right) && (6.10)\\
&= \operatorname{argmin}_{\boldsymbol{y}} \left\{ Y(\boldsymbol{y}) + \frac{\beta}{2} \left\| \mathbf{U}^s \boldsymbol{u}^{(k+1)} + \mathbf{Y}\boldsymbol{y} + \frac{1}{\beta}\boldsymbol{\rho}^{(k)} \right\|_2^2 \right\} && (6.11)\\
&= \operatorname{argmin}_{\boldsymbol{y}} \left\{ Y(\boldsymbol{y}) + \frac{\beta}{2} \left\| \boldsymbol{y} - \boldsymbol{v}^{(k)} \right\|_2^2 \right\}, \quad \boldsymbol{v}^{(k)} = \mathbf{U}^s \boldsymbol{u}^{(k+1)} + \frac{1}{\beta}\boldsymbol{\rho}^{(k)}, && (6.12)
\end{aligned}$$

$$\begin{aligned}
\boldsymbol{\rho}^{(k+1)} &= \boldsymbol{\rho}^{(k)} + \beta\left(\mathbf{U}^s \boldsymbol{u}^{(k+1)} + \mathbf{Y}\boldsymbol{y}^{(k+1)}\right), && (6.13)\\
&= \boldsymbol{\rho}^{(k)} + \beta\left(\mathbf{U}^s \boldsymbol{u}^{(k+1)} - \boldsymbol{y}^{(k+1)}\right), && (6.14)
\end{aligned}$$

where (6.8) and (6.11) follow easily from (6.7) and (6.10) by recalling the definition of $\mathcal{L}_\beta$ in (6.4), dropping the constant terms and carrying out some algebraic manipulations, whereas (6.9), (6.12) and (6.14) come immediately from (6.8), (6.11) and (6.13) after recalling from (6.2)-(6.3) that for our specific two-blocks separable minimization problem we have $U(\boldsymbol{u}) \equiv 0$ and $\mathbf{Y}$ equal to the negative identity matrix.

In the following Sections 6.1 and 6.2 we illustrate how the minimization subproblems (6.9) and (6.12) for primal variables $\boldsymbol{u}$ and $\boldsymbol{y}$ can be efficiently solved, respectively, then in Section 6.3 we outline the overall ADMM scheme and state its convergence.

The primal and dual residuals at iteration $k+1$ are defined ([8]), respectively, as

$$\boldsymbol{r}^{(k+1)} = \mathbf{U}^s \boldsymbol{u}^{(k+1)} - \boldsymbol{y}^{(k+1)}, \qquad \boldsymbol{s}^{(k+1)} = -\beta\left(\mathbf{U}^s\right)^{\mathrm{T}}\left(\boldsymbol{y}^{(k+1)} - \boldsymbol{y}^{(k)}\right).$$

Hence, we stop ADMM iterations as soon as both the primal and dual relative residual norms drop below some fixed thresholds:

$$\frac{\left\|\boldsymbol{r}^{(k+1)}\right\|_2}{\max\left\{\left\|\mathbf{U}^s \boldsymbol{u}^{(k)}\right\|_2, \left\|\boldsymbol{y}^{(k)}\right\|_2\right\}} < \epsilon_{\text{primal}}, \qquad \frac{\left\|\boldsymbol{s}^{(k+1)}\right\|_2}{\left\|\left(\mathbf{U}^s\right)^{\mathrm{T}} \boldsymbol{\rho}^{(k)}\right\|_2} < \epsilon_{\text{dual}}.$$

6.1. Solving the subproblem for $\boldsymbol{u}$

The Hessian matrix $\mathbf{H}^s$ of the quadratic cost function in (6.9) is given by

$$\mathbf{H}^s = \left(\mathbf{U}^s\right)^{\mathrm{T}} \mathbf{U}^s = \mathbf{I}_n + \left(\mathbf{D}^s\right)^{\mathrm{T}} \mathbf{D}^s \in \mathbb{R}^{n \times n},$$

with the second equality coming from the definition of matrix $\mathbf{U}^s$ in (6.3). Then, based on the definition of matrix $\mathbf{D}^s$ in (5.19), $\mathbf{H}^s$ reads

$$\mathbf{H}^s = \mathbf{I}_n + \left(\mathbf{D}_+^s\right)^{\mathrm{T}} \mathbf{D}_+^s + \left(\mathbf{D}_-^s\right)^{\mathrm{T}} \mathbf{D}_-^s. \tag{6.15}$$

Since the Hessian matrix $\mathbf{H}^s$ in (6.15) is clearly symmetric and positive definite (hence, non-singular), the quadratic cost function in (6.9) is strongly convex and, thus, admits a unique global minimizer coinciding with its unique stationary point. Hence, the updated vector $\boldsymbol{u}^{(k+1)}$ in (6.7) is obtained by solving the first-order optimality conditions for the minimization subproblem (6.9), that is by solving the linear system

$$\mathbf{H}^s \boldsymbol{u}^{(k+1)} = \mathbf{U}^{\mathrm{T}} \boldsymbol{q}^{(k)}, \tag{6.16}$$

with $\mathbf{H}^s$ in (6.15), $\mathbf{U}^s$ in (6.3) and $\boldsymbol{q}^{(k)}$ in (6.9). By assuming periodic boundary conditions for $\boldsymbol{u}$, the coefficient matrix $\mathbf{H}^s$ is circulant. Hence, the linear system in (6.16) can be solved very efficiently based on the discrete Fourier transform, implemented by 1d fast Fourier transform.

6.2. Solving the subproblem for $\boldsymbol{y}$

After recalling the definition of function Y in (6.2), it is easy to verify that the minimization problem for variable $\boldsymbol{y}$ in (6.12) is separable into two independent minimization subproblems for the subvectors $\boldsymbol{y}_1$ and $\boldsymbol{y}_2$. In formula, we have

$$\boldsymbol{y}^{(k+1)} = \begin{pmatrix} \boldsymbol{y}_1^{(k+1)} \\ \boldsymbol{y}_2^{(k+1)} \end{pmatrix} = \begin{pmatrix} \operatorname{argmin}_{\boldsymbol{y}_1} \left\{ \frac{1}{\beta} \|\boldsymbol{y}_1\|_1 + \frac{1}{2} \left\| \boldsymbol{y}_1 - \boldsymbol{v}_1^{(k)} \right\|_2^2 \right\} \\ \operatorname{argmin}_{\boldsymbol{y}_2} \left\{ \frac{\lambda}{\beta} \|\boldsymbol{y}_2 - \boldsymbol{g}\|_1 + \frac{1}{2} \left\| \boldsymbol{y}_2 - \boldsymbol{v}_2^{(k)} \right\|_2^2 \right\} \end{pmatrix}, \tag{6.17}$$

where we introduced the following suitable partitions of vector $\boldsymbol{v}^{(k)}$ in (6.12) and of vector $\boldsymbol{\rho}^{(k)}$ of Lagrange multipliers,

$$\boldsymbol{v}^{(k)} = \begin{pmatrix} \boldsymbol{v}_1^{(k)} \\ \boldsymbol{v}_2^{(k)} \end{pmatrix} = \begin{pmatrix} \mathbf{D}^s \boldsymbol{u}^{(k+1)} + \frac{1}{\beta} \boldsymbol{\rho}_1^{(k)} \\ \boldsymbol{u}^{(k+1)} + \frac{1}{\beta} \boldsymbol{\rho}_2^{(k)} \end{pmatrix}, \qquad \boldsymbol{\rho}^{(k)} = \begin{pmatrix} \boldsymbol{\rho}_1^{(k)} \\ \boldsymbol{\rho}_2^{(k)} \end{pmatrix},$$

with $\boldsymbol{v}_1^{(k)}, \boldsymbol{\rho}_1^{(k)} \in \mathbb{R}^{2n}$ and $\boldsymbol{v}_2^{(k)}, \boldsymbol{\rho}_2^{(k)} \in \mathbb{R}^n$. It is immediate to verify that, after the change of variable $\widetilde{\boldsymbol{y}}_2 = \boldsymbol{y}_2 - \boldsymbol{g}$, the update formula for $\boldsymbol{y}_2$ in (6.17) can be equivalently written as

$$\boldsymbol{y}_2^{(k+1)} = \boldsymbol{g} + \operatorname{argmin}_{\widetilde{\boldsymbol{y}}_2} \left\{ \frac{\lambda}{\beta} \|\widetilde{\boldsymbol{y}}_2\|_1 + \frac{1}{2} \left\| \widetilde{\boldsymbol{y}}_2 - \left(\boldsymbol{v}_2^{(k)} - \boldsymbol{g} \right) \right\|_2^2 \right\}. \tag{6.18}$$

The minimization problems for $\boldsymbol{y}_1$ in (6.17) and for $\widetilde{\boldsymbol{y}}_2$ in (6.18) have the same form and correspond to the proximity operator of the scaled ℓ_1-norm function $\alpha\|\cdot\|_1$ evaluated at point $\boldsymbol{z}$, with $\alpha = 1/\beta$, $\boldsymbol{z} = \boldsymbol{v}_1^{(k)}$ and $\alpha = \lambda/\beta$, $\boldsymbol{z} = \boldsymbol{v}_2^{(k)} - \boldsymbol{g}$, respectively. Hence, based on the well-known closed-form solution to such a proximity operator (vectorial soft-threshold function), we get the following explicit updating formula for variable $\boldsymbol{y}$:

$$\boldsymbol{y}^{(k+1)} = \begin{pmatrix} \boldsymbol{y}_1^{(k+1)} \\ \boldsymbol{y}_2^{(k+1)} \end{pmatrix} = \begin{pmatrix} \operatorname{sign}\left(\boldsymbol{v}_1^{(k)} \right) \odot \max \left\{ \left| \boldsymbol{v}_1^{(k)} \right| - \frac{1}{\beta}, 0 \right\} \\ \operatorname{sign}\left(\boldsymbol{v}_2^{(k)} - \boldsymbol{g} \right) \odot \max \left\{ \left| \boldsymbol{v}_2^{(k)} - \boldsymbol{g} \right| - \frac{\lambda}{\beta}, 0 \right\} + \boldsymbol{g} \end{pmatrix}, \tag{6.19}$$

where $\odot$ denotes the Hadamard vector product and the sign and max operators have to be intended component-wise.

6.3. The overall convergent ADMM scheme

In Algorithm 1 we report the main computational steps of the iterative ADMM scheme described in detail in previous sections and used for solving the proposed denoising model (5.17)-(5.18).

Algorithm 1: ADMM scheme to solve the denoising model in (5.17)-(5.18).

inputs: observed noisy signal $\boldsymbol{g} \in \mathbb{R}^n$,
model parameters $s, \lambda \in \mathbb{R}_{++}$
output: estimated denoised signal $\widehat{\boldsymbol{u}}(s, \lambda) \in \mathbb{R}^n$

1. **initialize:** set $\boldsymbol{u}^{(0)} = \boldsymbol{g}$, $\boldsymbol{y}^{(0)} = \mathbf{U}^s \boldsymbol{u}^{(0)}$, $\boldsymbol{\rho}^{(0)} = \mathbf{0}$
2. **for** $k = 0, 1, 2, \ldots$ *until convergence* **do**:
3. · compute $\boldsymbol{u}^{(k+1)}$ by solving the linear system in (6.15)-(6.16)
4. · compute $\boldsymbol{y}^{(k+1)}$ by using the explicit formula in (6.19)
5. · compute $\boldsymbol{\rho}^{(k+1)}$ by using the explicit formula in (6.14)
6. **end for**
7. $\widehat{\boldsymbol{u}}(s, \lambda) = \boldsymbol{u}^{(k+1)}$

The performance of the two-blocks ADMM algorithm is highly sensitive to the choice of the dual step-size β in (6.14). In the convex setting, under standard assumptions on the two cost functions $U(u)$, $Y(y; \lambda)$ and on the linear constraint $\mathrm{U}\boldsymbol{u} + \mathrm{Y}\boldsymbol{y} = 0$, the step-size β primarily influences the convergence rate. To improve the convergence rate of the proposed ADMM scheme, we follow the results in [46]. More precisely, in (6.14) we use an iteration-adaptive step-size β_k which, according to the proposal in [46], is updated at each ADMM iteration as follows:

$$\beta_{k+1} = (1 - \omega_k)\beta_k + \omega_k \operatorname{proj}_{[\beta_m, \beta_M]} \left(\frac{\|\boldsymbol{\rho}^{(k+1)}\|_2}{\|\boldsymbol{y}^{(k+1)}\|_2} \right), \ \omega_k \in (0, 1), \tag{6.20}$$

with $0 < \beta_m < \beta_M < \infty$, and $\omega_k \in (0, 1]$ a summable "conservation sequence" with $\omega_0 = 1$. As a consequence, the sequence $\{\rho_k\}$ generated by the ADMM scheme using the dual step-size updating rule in (6.20) weakly converges to a solution of the dual problem, then the ADMM convergence is guaranteed, as outlined in [46].

To conclude, in the following Proposition 6.1 we apply to the ADMM scheme in Algorithm 1 a general and classical convergence result for the two-blocks ADMM given in the seminal paper by Eckstein and Bertsekas [24].

Proposition 6.1. *Let $\mathcal{L}$, $\mathcal{L}_\beta$ be the Lagrangian and the augmented Lagrangian functions in (6.4)-(6.5) with functions U, Y and matrices $\mathbf{U}^s$, $\mathbf{Y}$ defined as in (6.2)-(6.3). Then, if a saddle point of $\mathcal{L}$ exists, the ADMM scheme in Algorithm 1 converges to a saddle point $\{\widehat{\boldsymbol{u}}(s,\lambda), \widehat{\boldsymbol{y}}(s,\lambda), \widehat{\boldsymbol{\rho}}(s,\lambda)\}$ of $\mathcal{L}_\beta$ for any $s,\lambda,\beta \in \mathbb{R}_{++}$ and any data $\boldsymbol{g} \in \mathbb{R}^n$, with $\widehat{\boldsymbol{u}}(s,\lambda)$ a solution of the minimization problem in (5.17). If a saddle point of $\mathcal{L}$ does not exist, then at least one of the two sequences of ADMM iterates $\{\boldsymbol{y}^{(k)}\}$ or $\{\boldsymbol{\rho}^{(k)}\}$ is unbounded.*

Proof. For any $s,\lambda \in \mathbb{R}_{++}$ and any data $\boldsymbol{g} \in \mathbb{R}^n$, the functions U, Y defined in (6.2) are both clearly proper, closed and convex and the matrices $\mathbf{U}^s$, $\mathbf{Y}$ defined in (6.3) are such that $\mathbf{Y}$ is the negative identity and $\mathbf{U}^s$ has full (column) rank. Moreover, the two ADMM minimization subproblems for the primal variables $\boldsymbol{u}$ and $\boldsymbol{y}$ are solved exactly based on formulas in (6.15)-(6.16) and (6.19), respectively. Hence, by applying the classical convergence result for the two-blocks ADMM given in [24] (Theorem 8), the proof of the statement follows easily. □

7. Automatic joint selection of parameters (s,λ) by the whiteness principle

Very recently, it has been proposed in [30] the so-called Multi-parameter Residual Whiteness Principle (in short, MRWP) applied to the automatic selection of the pair of free parameters in a specific variational model for the restoration - i.e., deblurring and denoising - of images corrupted by space-invariant blur and additive white Gaussian noise. The MRWP represents the first attempt to extend to the multi-parametric case the so-called Residual Whiteness Principle (RWP), proposed in [31,32] for the selection of a single parameter in a class of variational models for image restoration under additive white Gaussian noise corruptions. However, both the single-parameter RWP in [31] and the multi-parameter MRWP in [30] not only have been proposed for models containing an L^2 data fidelity term and experimentally validated for the specific case of Gaussian-distributed noise but, more importantly, have been applied to models where the parameter(s) to select enter linearly the optimized cost function.

In the following, we introduce a formal definition of the MRWP applied to the selection of the pair of free parameters (s,λ) in our variational model (5.17), where an L^1 - instead of L^2 - fidelity term is present and where, for the first time, one of the parameters to select - namely, s - enters the optimized cost function non-linearly.

When applied to our discrete model in (5.17), the idea of the MRWP is to select the pair of parameters $(s,\lambda) \in \mathbb{R}^2_{++}$ so that the residual 1d signal $\widehat{\boldsymbol{r}}(s,\lambda)$ associated to the model solution $\widehat{\boldsymbol{u}}(s,\lambda)$, defined by

$$\widehat{\boldsymbol{r}}(s,\lambda) := \boldsymbol{g} - \widehat{\boldsymbol{u}}(s,\lambda), \tag{7.1}$$

is maximally white (uncorrelated). In fact, if the model solution $\widehat{\boldsymbol{u}}(s,\lambda)$ is a good estimate of the target noise-free signal, then the associated residual signal $\widehat{\boldsymbol{r}}(s,\lambda)$ in (7.1) is a good estimate of the realization of the corrupting noise, which in this work is assumed to be additive white Laplacian-distributed. By maximizing whiteness of the residual signal in (7.1), we hope to minimize the distance between the estimated signal $\widehat{\boldsymbol{u}}(s,\lambda)$ and the target noise-free signal.

Following [30], the MRWP applied to our model reads

$$\text{Select } (s,\lambda) = (\hat{s},\hat{\lambda}) \in \operatorname{argmin}_{(s,\lambda)\in\mathbb{R}^2_{++}} W(s,\lambda),$$

with the multi-parameter whiteness measure function $W : \mathbb{R}^2_{++} \to \mathbb{R}_+$ defined by the squared Euclidean norm of the 1d discrete normalized auto-correlation of the residual,

$$W(s,\lambda) := \frac{\|\widehat{\boldsymbol{r}}(s,\lambda) \bigstar \widehat{\boldsymbol{r}}(s,\lambda)\|_2^2}{\|\widehat{\boldsymbol{r}}(s,\lambda)\|_2^4} = \frac{\|\big(\boldsymbol{g} - \widehat{\boldsymbol{u}}(s,\lambda)\big) \bigstar \big(\boldsymbol{g} - \widehat{\boldsymbol{u}}(s,\lambda)\big)\|_2^2}{\|\big(\boldsymbol{g} - \widehat{\boldsymbol{u}}(s,\lambda)\big)\|_2^4}, \tag{7.2}$$

where the second equality comes from using definition (7.1) and where $\bigstar$ indicates the 1d discrete cross-correlation operator: $\mathbf{a} \bigstar \mathbf{b} := \sum_{h\in\mathbb{Z}} \overline{\mathbf{a}}_h \mathbf{b}_{k+h}$.

By assuming a periodic extension $\widetilde{r}$ of the residual signal $\widehat{\boldsymbol{r}}(s,\lambda)$, function $W(s,\lambda)$ in (7.2) can be equivalently written in terms of $\widetilde{\widehat{\boldsymbol{r}}}(s,\lambda)$, the 1d discrete Fourier transformed version of $\widehat{\boldsymbol{r}}(s,\lambda)$, as follows

$$W(s,\lambda) = \frac{\displaystyle\sum_{i=1}^{n} w_i^4(s,\lambda)}{\left(\displaystyle\sum_{i=1}^{n} w_i^2(s,\lambda)\right)^2}, \quad \text{with } w_i(s,\lambda) := \left|\widetilde{\widehat{r}}_i(s,\lambda)\right|, \tag{7.3}$$

where $\widetilde{\widehat{r}}_i(s,\lambda) \in \mathbb{C}$ is the i-th component of $\widetilde{\widehat{\boldsymbol{r}}}(s,\lambda)$ and $|\cdot|$ indicates the modulus.

Due (also) to non-smoothness of the cost function G, neither the solution $\widehat{\boldsymbol{u}}(s,\lambda)$ of our model in (5.17), nor the associated residual signal $\widehat{\boldsymbol{r}}(s,\lambda)$ defined as in (7.1) can be written as explicit functions of the pair of parameters (s,λ). Therefore, we apply the MRWP outlined above *a posteriori*: we compute the solution $\widehat{\boldsymbol{u}}(s,\lambda)$ - and, then, the residual $\widehat{\boldsymbol{r}}(s,\lambda)$ - of model (5.17) for different values $(s,\lambda) \in \mathbb{R}^2_{++}$ selected on a (pre-defined or adaptively-defined) 2d grid and then calculate the corresponding whiteness measures $W(s,\lambda)$ by (7.2) or, equivalently, (7.3). The optimal pair $(\hat{s},\hat{\lambda})$ is then selected as the one minimizing $W(s,\lambda)$ on the chosen discrete grid.

8. Numerical examples

In this section, we perform a qualitative and quantitative experimental evaluation of the proposed variational model for denoising 1d signals corrupted by additive white Laplace noise. We also aim to test the effectiveness of the proposed automatic whiteness-based strategy for selecting the "best" couple of fractional order parameter s and regularization parameter λ. All tests have been performed in Matlab R2022b.

In order to measure the quality of the denoised signals $\widehat{\boldsymbol{u}}(s,\lambda)$, with respect to the target uncorrupted signal $\bar{\boldsymbol{u}}$ obtained by model (5.17) for varying parameters $(s,\lambda)\in\mathbb{R}^2_{++}$ we use two different well-known quality assessment metrics, namely the relative error (RELERR), and the structure similarity index measure (SSIM), defined by

$$\mathrm{RELERR}\,(s,\lambda) := \frac{\left\|\widehat{\boldsymbol{u}}(s,\lambda)-\bar{\boldsymbol{u}}\right\|_2}{\|\bar{\boldsymbol{u}}\|_2}\,, \tag{8.1}$$

$$\mathrm{SSIM}\,(s,\lambda) := L\left(\widehat{\boldsymbol{u}}(s,\lambda),\bar{\boldsymbol{u}}\right)\cdot C\left(\widehat{\boldsymbol{u}}(s,\lambda),\bar{\boldsymbol{u}}\right)\cdot S\left(\widehat{\boldsymbol{u}}(s,\lambda),\bar{\boldsymbol{u}}\right)\,, \tag{8.2}$$

where SSIM in (8.2) is the product of three terms, namely the *luminance* term L, the *contrast* term C and the *structure* term S. A value closer to 1 indicates better signal quality. The SSIM metric in (8.2) is computed by the Matlab routine `ssim`.

We consider four different 1d signals, whose discrete versions are referred to as $\bar{\boldsymbol{u}}_1$, $\bar{\boldsymbol{u}}_2$, $\bar{\boldsymbol{u}}_3$ and $\bar{\boldsymbol{u}}_4$, characterized by being discontinuous piecewise constant, discontinuous piecewise affine, continuous piecewise affine and smooth, respectively. The four signals are reported (solid red lines) in both the graphs in the top rows of Figs. 2, 3, 4, 5, respectively. All signals are made of 256 samples but $\bar{\boldsymbol{u}}_4$ which contains 200 samples.

All the four signals $\bar{\boldsymbol{u}}_1$, $\bar{\boldsymbol{u}}_2$, $\bar{\boldsymbol{u}}_3$ and $\bar{\boldsymbol{u}}_4$ have been synthetically corrupted by different realizations $\boldsymbol{e}_1$, $\boldsymbol{e}_2$, $\boldsymbol{e}_3$ and $\boldsymbol{e}_4$ of additive white Laplace noise with zero-mean and different standard deviations σ_1, σ_2, σ_3, σ_4 (specified in the captions of the figures reported), thus obtaining the four noise-corrupted signals

$$\boldsymbol{g}_i = \bar{\boldsymbol{u}}_i + \boldsymbol{e}_i\,,\quad i=1,2,3,4\,.$$

The noisy signals are shown (solid blue lines) in the top-left graphs of Figs. 2, 3, 4, 5.

Then, for each of the four cases, we defined a grid of parameter couples (s_j,λ_k) and, for every couple, we ran the proposed ADMM optimization algorithm to get the associated denoised signals $\widehat{\boldsymbol{u}}_i(s_j,\lambda_k)$ and the two corresponding quality metrics defined in (8.1)-(8.2). The two quality metric surfaces are shown in the left columns of Figs. 2, 3, 4, 5. The yellow and blue dots on the surfaces indicate the "best" achieved denoising results according to the two metrics in (8.1)-(8.2), respectively.

In order to test the effectiveness of the proposed whiteness-based strategy for automatically selecting the parameter couple (s,λ), for each estimated denoised image $\widehat{\boldsymbol{u}}_i(s_j,\lambda_k)$ we also compute the associated value of the whiteness measure function $W(s_j,\lambda_k)$ defined in (7.2). The four whiteness measure surfaces obtained are reported in the bottom-left panel of Figs. 2, 3, 4, 5. The red dots in the surface plots of Figs. 2, 3, 4, 5 (left panel) indicate the global minima of the whiteness measures. The corresponding denoised signals are shown (solid black lines) in the right-columns of Figs. 2, 3, 4, 5. In Fig. 6 we show for comparison the denoised signals obtained by minimizing the functional composed by the sum of the standard TV regularizer with L^1 fidelity term, which we named TV-L^1 model.

The reported experimental results strongly indicate that, independently of the regularity of the target uncorrupted signal, (a) the proposed whiteness-based criterion works very well for selecting a "nearly optimal" couple of parameters (s,λ) in the proposed model and is much better for smooth targets, (b) the proposed SFV-L^1 model holds the potential to achieve high-quality denoising results, and (c) the degree of freedom encoded in the order s of fractional derivatives in our model enables the attainment of substantially more compelling outcomes than those achieved by the standard TV-L^1 model. It is worth highlighting that the size of the signals can affect the power of the whiteness-based criterion. In fact, the larger the size of signals, the more reliable the statistical principle at the basis of the criterion will be.

A deeper analysis of the results obtained allows us to highlight how the estimated values of the fractional order parameter s are, in the four experiments, all consistent with the different regularities of the target signals. In particular, for piecewise constant, piecewise affine and for smooth target signals like $\bar{\boldsymbol{u}}_1$, $\bar{\boldsymbol{u}}_3$ and $\bar{\boldsymbol{u}}_4$ (see Figs. 2, 4 and 5, respectively) it is well-known that promoting sparsity of the first-order derivatives, second-order derivatives and high-order derivatives of the reconstructed signal is a successful strategy in variational signal denoising. For more complex signals exhibiting geometrical properties which vary in their domain, like $\bar{\boldsymbol{u}}_2$ in Fig. 2, using a unique s-value in the fractional variational model can represent a limitation yielding sub-optimal denoising results. This issue will be the subject of future research.

To highlight the advantages of the proposed symmetrized regularizer with respect to the one-sided versions of it and to the TV-L^1 model, we report in Table 2 the achieved quality metrics associated to the denoising results for all considered signals $\bar{\boldsymbol{u}}_1$, $\bar{\boldsymbol{u}}_2$, $\bar{\boldsymbol{u}}_3$ and $\bar{\boldsymbol{u}}_4$ shown in Figs. 2, 3, 4, 5. The accuracy of the results we obtained by using the proposed SFV-L^1 model is slightly higher both in terms of RELERR and in terms of SSIM.

In order to provide experimental evidence of the importance to select an s-value consistent with the target signal regularity, in Fig. 7 we report, for the last (smooth) signal experiment, the "best" denoised signals obtained by using five different values of s (that is, for each s, we consider the best achievable denoised signal in terms of RELERR by letting λ vary).

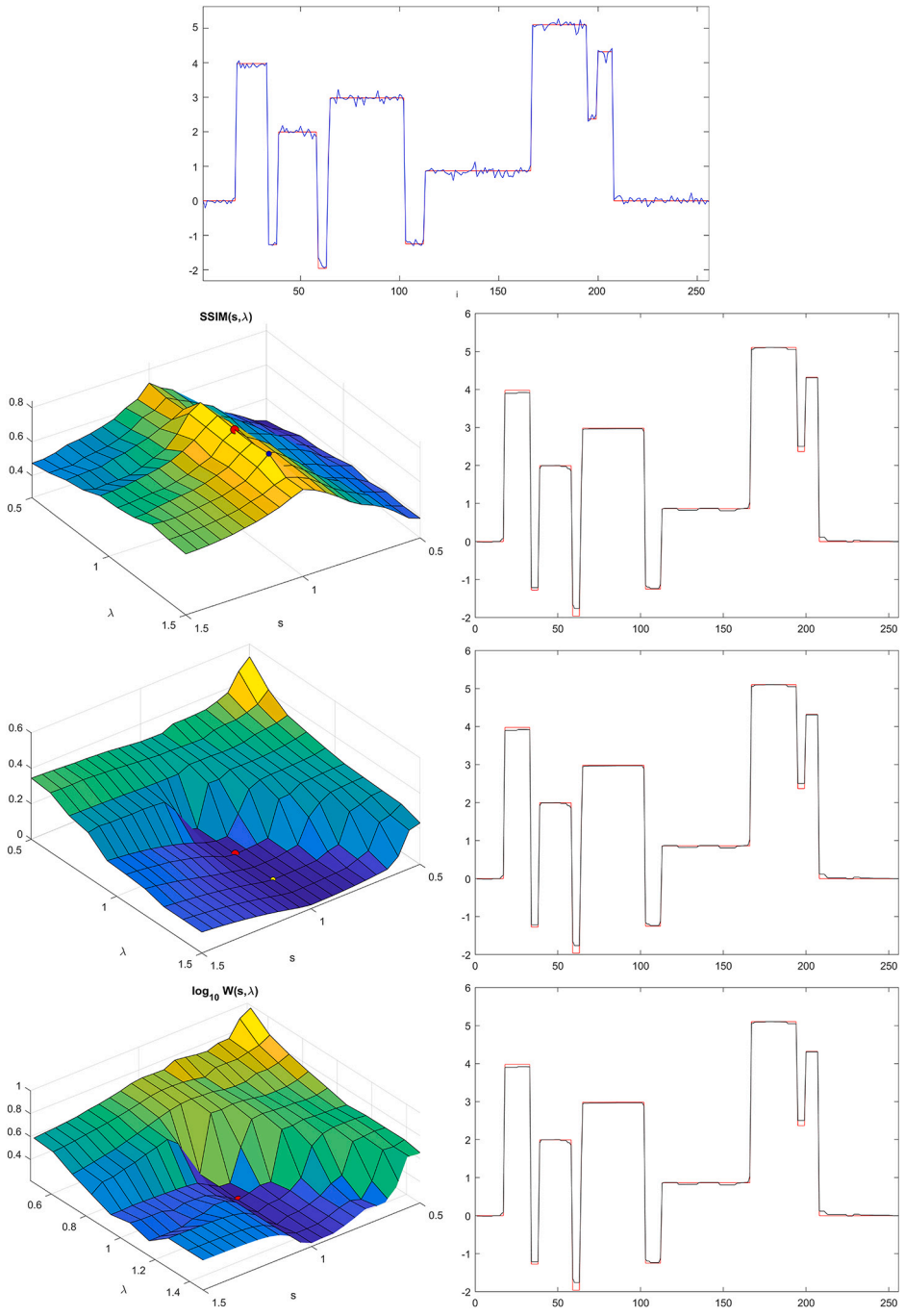

Fig. 2. $\bar{\boldsymbol{u}}_1$ discontinuous piecewise constant signal: denoising results, $n = 256$, for different values of λ and s, additive white Laplace noise $\sigma_1 = 0.1$. Best denoised signal obtained with RELERR(s, λ) = 0.02 ($s = 1.0$, $\lambda = 1.28$), versus RELERR(s, λ) = 0.02 selected by WP ($s = 1.0$, $\lambda = 1.06$); SSIM(s, λ) = 0.84 ($s = 1.0$, $\lambda = 1.28$) (versus SSIM(s, λ) = 0.83 selected by WP).

9. Conclusions

We propose a novel variational model, named SFV-L^1, for signal denoising. The model exploits regularizing terms involving both right and left Riemann-Liouville fractional derivatives, aiming for an orientation-independent approach, together with an L^1-norm data-fitting term. The proposed variational model addresses the artifact problems inherent in the classical total variation regularization approach, offering a more effective denoising solution for signals corrupted by additive white Laplace noise. To ensure accurate model representation, we employed a second-order consistent discretization scheme based on a truncated Grünwald-Letnikov approximation for the fractional derivatives in 1d. This scheme was then solved efficiently using a convergent, iterative ADMM-based algorithm.

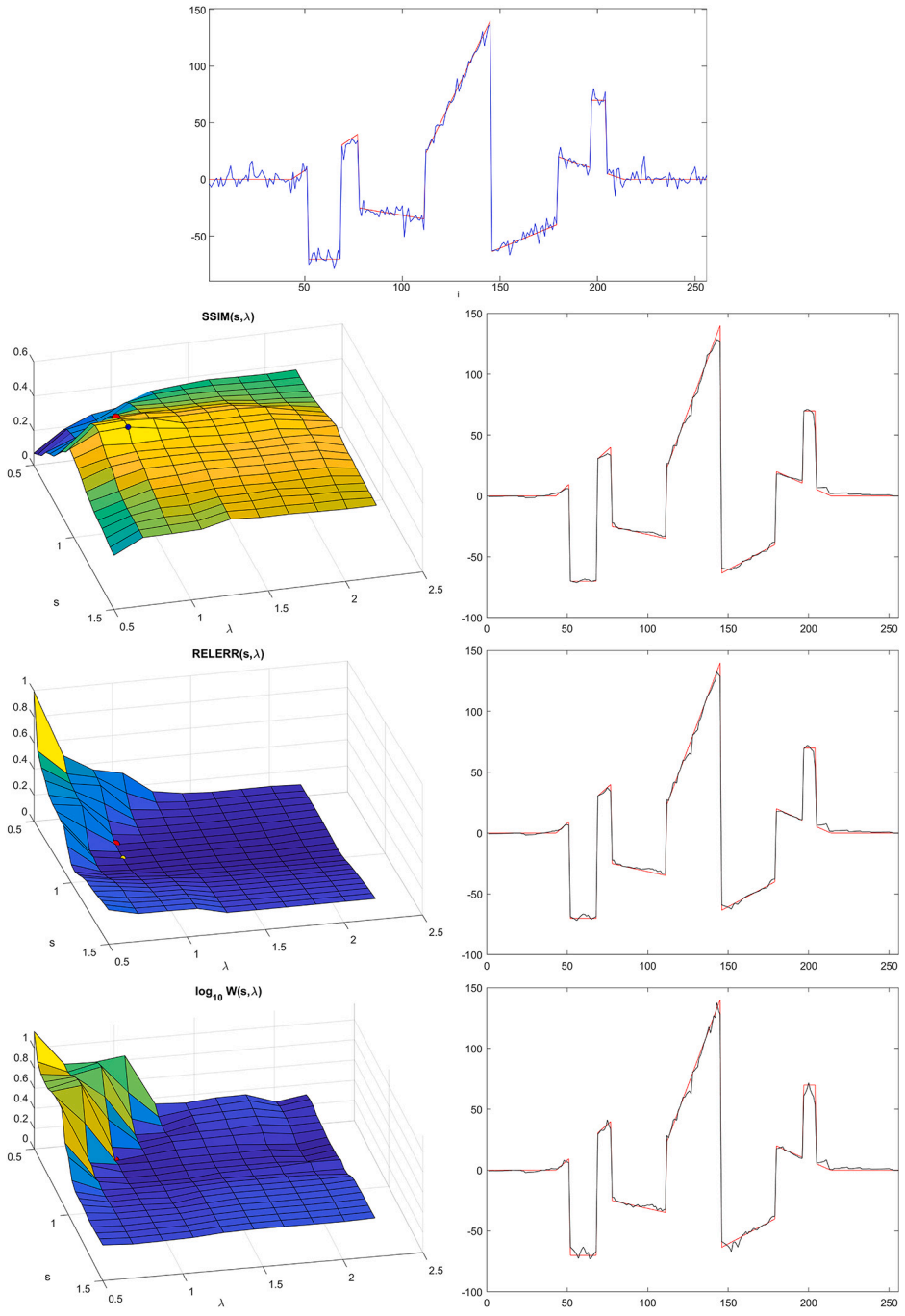

Fig. 3. $\bar{\boldsymbol{u}}_2$ discontinuous piecewise affine signal: denoising results, $n = 256$, for different values of λ and s, additive white Laplace noise $\sigma_2 = 5$. Best denoised signal obtained with RELERR(s, λ) = 0.05 ($s = 0.9$, $\lambda = 0.88$), versus RELERR(s, λ) = 0.06 selected by WP ($s = 0.8$, $\lambda = 0.88$); SSIM(s, λ) = 0.55 ($s = 0.95$, $\lambda = 0.88$) (versus SSIM(s, λ) = 0.48 selected by WP).

Numerical experiments on 1d signals validated the proposed model's ability to denoise 1d signals corrupted by additive Laplace noise, independently on their degree of regularity, from discontinuous piecewise constant, discontinuous piecewise affine, continuous piecewise affine and smooth.

Another key contribution of this work is the development of a multi-parameter whiteness criterion. This criterion automates the selection of two crucial parameters in the model, the fractional order for the regularizer and the fidelity parameter, eliminating the need for manual tuning. In conclusion, this work introduces the SFV-L^1 variational model for signal and image analysis. The model's effectiveness for denoising signals with Laplace noise is demonstrated. Future research directions include extending the model to textured image restoration and developing a comprehensive functional analysis for the model with general parameter values ($s \geq 1$).

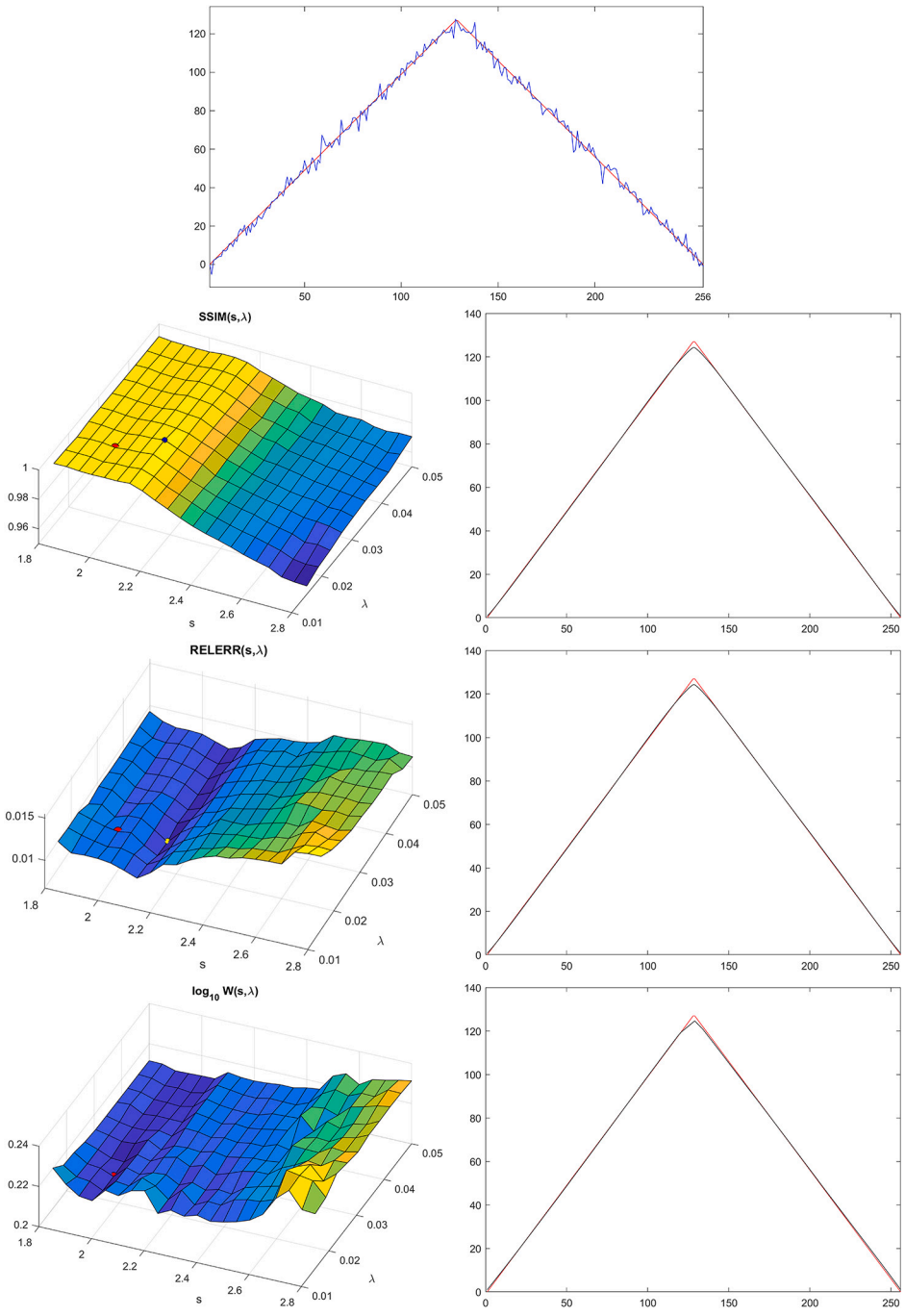

Fig. 4. $\bar{u}_3$ continuous piecewise affine and smooth signal: denoising results, $n = 256$, for different values of λ and s, additive white Laplace noise $\sigma_3 = 3$. Best denoised signal obtained with RELERR(s, λ) = 0.007 ($s = 2.10$, $\lambda = 0.03$), versus RELERR(s, λ) = 0.008 selected by WP ($s = 1.95$, $\lambda = 0.02$); SSIM(s, λ) = 0.993 ($s = 2.10$, $\lambda = 0.03$) (versus SSIM(s, λ) = 0.990 selected by WP).

Funding

The authors Antonio Leaci and Franco Tomarelli are members of Gruppo Nazionale per l'Analisi Matematica, la Probabilità e le loro Applicazioni (GNAMPA) of the Istituto Nazionale di Alta Matematica (INdAM). Alessandro Lanza and Serena Morigi are members of Gruppo Nazionale di Calcolo Scientifico (GNCS) of the Istituto Nazionale di Alta Matematica (INdAM).
Antonio Leaci is partially funded by the Italian M.U.R. PRIN grant number 20223L2NWK "Elliptic and parabolic problems, heat kernel estimates and spectral theory".

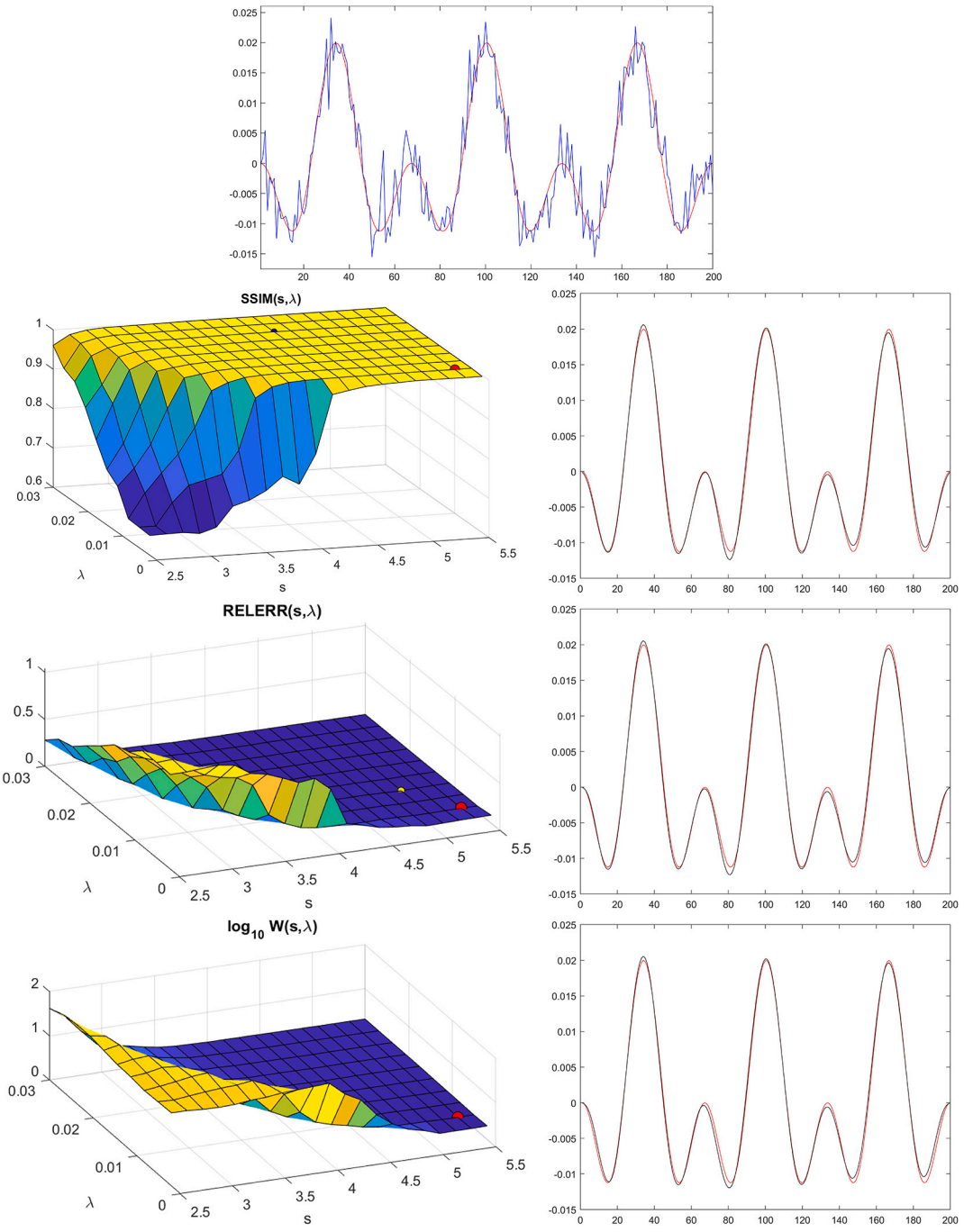

Fig. 5. $\bar{u}_4$ smooth signal: denoising results, $n = 200$, for different values of λ and s, additive white Laplace noise $\sigma_4 = 0.003$. Best denoised signal obtained with RELERR(s, λ) = 0.051 ($s = 5.05$, $\lambda = 0.01$), versus RELERR(s, λ) = 0.062 selected by WP ($s = 5.35$, $\lambda = 0.005$); SSIM(s, λ) = 0.998 ($s = 4.3$, $\lambda = 0.02$) (versus SSIM(s, λ) = 0.998 selected by WP).

Franco Tomarelli is partially funded from the INdAM/GNAMPA 2023 Project Codice CUP_ E53C22001930001, “Modelli variazionali ed evolutivi per problemi di adesione e di contatto” and by PRIN 2022 (Project no. 2022J4FYNJ), funded by MUR, Italy, and the European Union – Next Generation EU, Mission 4 Component 1 CUP F53D23002760006. Serena Morigi has been supported in part by the GNCS INdAM, Research Projects 2024. The work of Serena Morigi and Alessandro Lanza was supported by PRIN2022_MORIGI, titled “Inverse Problems in the Imaging Sciences (IPIS)” 2022 ANC8HL - CUP J53D23003670006, and PRIN2022_PNRR_CRESCENTINI CUP J53D23014080001. Serena Morigi is supported by MICS (Made in Italy – Circular and Sustain-

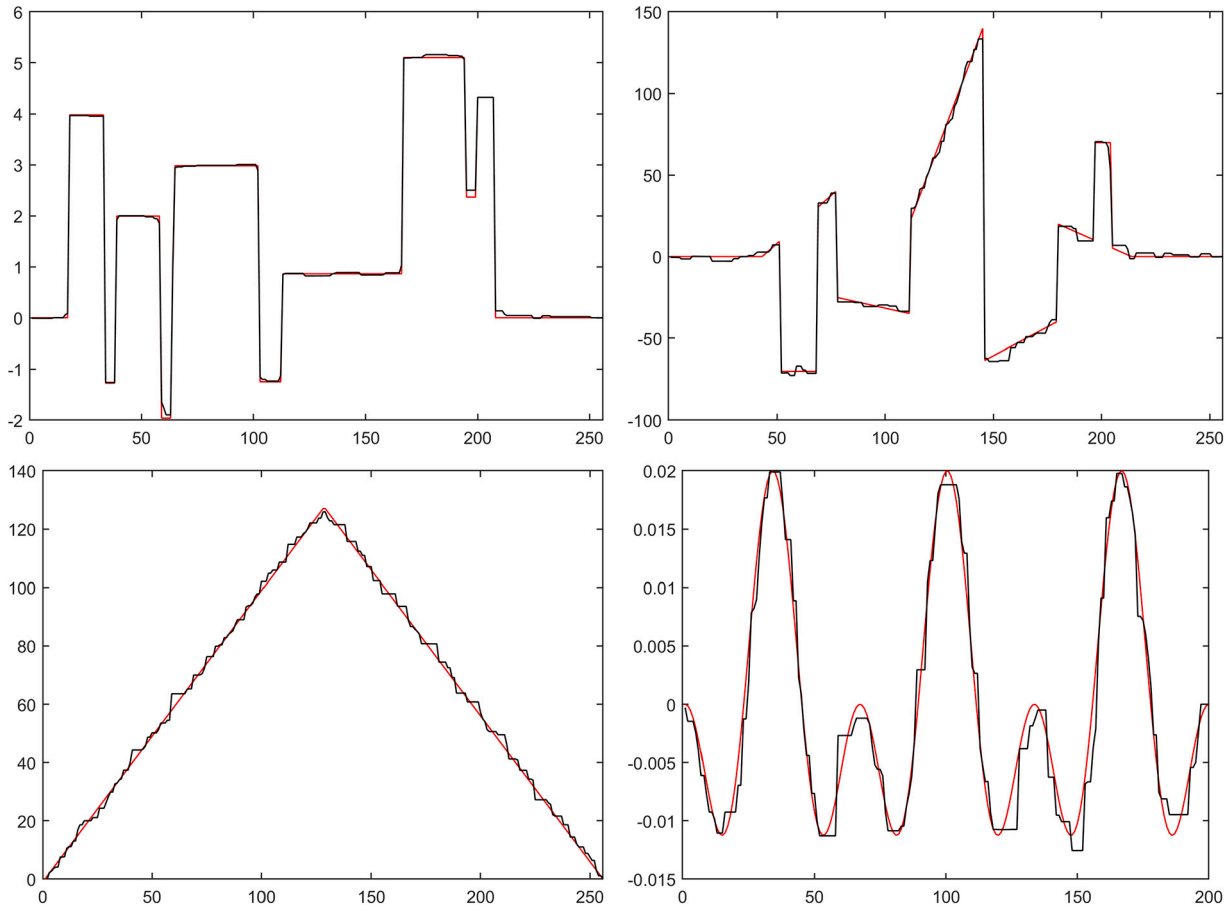

Fig. 6. Denoising results for the signals $\bar{\boldsymbol{u}}_1$-$\bar{\boldsymbol{u}}_4$ by applying TV-L^1 model, $n = 256$, for the optimal value of λ.

Table 2
Quantitative comparison of the quality metrics for the symmetrized (see (5.18)), one-sided versions $\mathrm{FV}_{\pm} := \left\| \mathbf{D}^s_{\pm} \mathbf{u} \right\|_1$ of the fractional regularizer and TV regularizer. All the models are equipped with the same L^1 fidelity.

	RELERR				SSIM			
	$\bar{\boldsymbol{u}}_1$	$\bar{\boldsymbol{u}}_2$	$\bar{\boldsymbol{u}}_3$	$\bar{\boldsymbol{u}}_4$	$\bar{\boldsymbol{u}}_1$	$\bar{\boldsymbol{u}}_2$	$\bar{\boldsymbol{u}}_3$	$\bar{\boldsymbol{u}}_4$
SFV	0.0211	0.0508	0.0067	0.0519	0.8390	0.5564	0.9932	0.9987
FV_+	0.0222	0.0581	0.0085	0.0962	0.6706	0.4841	0.9897	0.9953
FV_-	0.0222	0.0604	0.0095	0.0952	0.6624	0.4562	0.9879	0.9953
TV	0.0186	0.0537	0.0219	0.1731	0.8113	0.4781	0.7528	0.9900

able) European Union Next-GenerationEU (PNRR) – MISSIONE 4 COMPONENTE 2, INVESTIMENTO 1.3 – D.D. 1551.11-10-2022, PE00000004 CUP J33C22002950001, and by HPC National Centre for HPC, Big Data and Quantum Computing - CN00000013, CUP J33C22001170001.

Data availability

No data was used for the research described in the article.

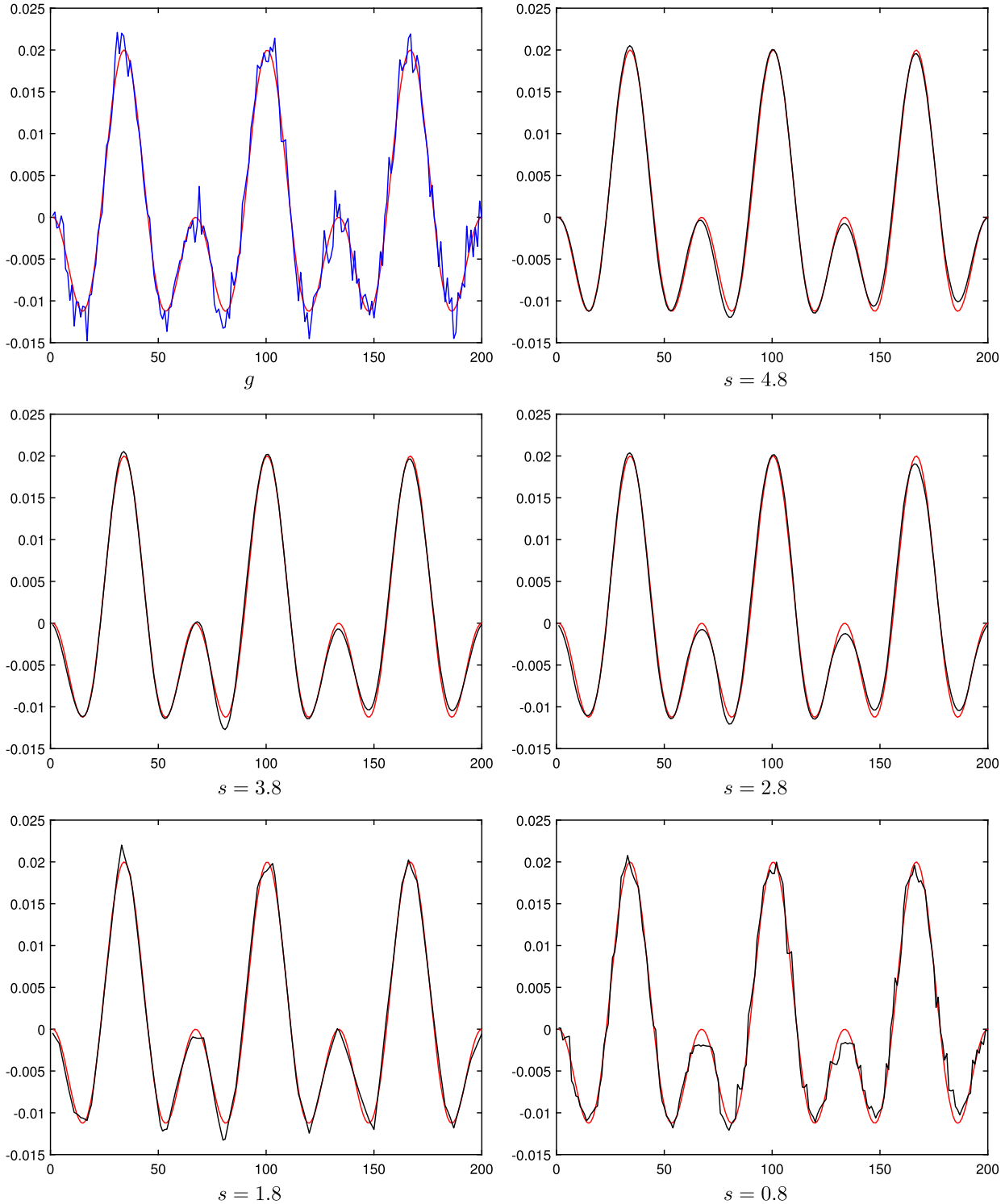

Fig. 7. $\bar{\boldsymbol{u}}_4$ smooth signal: best denoising results (that is, the best achievable by letting λ vary) for a signal g perturbed with additive white Laplace noise $\sigma_4 = 0.002$: RELERR$(\widehat{\boldsymbol{u}}_4(4.8, 0.006), \bar{\boldsymbol{u}}_4) = 0.003$, RELERR$(\widehat{\boldsymbol{u}}_4(3.8, 0.04), \bar{\boldsymbol{u}}_4) = 0.055$, RELERR$(\widehat{\boldsymbol{u}}_4(2.8, 0.16), \bar{\boldsymbol{u}}_4) = 0.067$ RELERR$(\widehat{\boldsymbol{u}}_4(1.8, 0.621), \bar{\boldsymbol{u}}_4) = 0.074$ RELERR$(\widehat{\boldsymbol{u}}_4(0.8, 1.100), \bar{\boldsymbol{u}}_4) = 0.1176$.

References

[1] S. Alliney, S.A. Ruzinsky, An algorithm for the minimization of mixed l_1 and l_2 norms with application to Bayesian estimation, Trans. Signal Process. 42 (3) (1994) 618–627.
[2] M. Amar, V. De Cicco, The uniqueness as a generic property for some one dimensional segmentation problems, Rend. Semin. Mat. Univ. Padova 88 (1992) 151–173.
[3] M. Bergounioux, A. Leaci, G. Nardi, F. Tomarelli, Fractional Sobolev spaces and functions of bounded variation of one variable, Fract. Calc. Appl. Anal. 20 (4) (2017) 936–962.
[4] K. Bessas, Fractional total variation denoising model with L1 fidelity, Nonlinear Anal. 222 (2022) 112926.
[5] K. Bessas, G. Stefani, Non-local BV functions and a denoising model with L^1 fidelity, preprint, 2022.
[6] T. Boccellari, F. Tomarelli, Generic uniqueness of minimizer for Blake & Zisserman functional, Rev. Mat. Complut. 26 (2013) 361–408.
[7] V.I. Bogachev, Measure Theory, vol. I, 2007th edition, Springer, Berlin, 2006.
[8] S. Boyd, N. Parikh, E. Chu, B. Peleato, J. Eckstein, Distributed optimization and statistical learning via the alternating direction method of multipliers, Found. Trends Mach. Learn. 3 (1) (2011) 1–122.
[9] K. Bredies, K. Kunisch, T. Pock, Total generalized variation, SIAM J. Imaging Sci. 3 (3) (2010) 492–526.
[10] H. Brezis, Functional Analysis, Sobolev Spaces and Partial Differential Equations, Universitext, Springer, New York, 2011.
[11] A. Carbotti, G.E. Comi, A note on Riemann-Liouville fractional Sobolev spaces, Commun. Pure Appl. Anal. 20 (1) (2021) 17–54.
[12] M. Carriero, A. Leaci, F. Tomarelli, A second order model in image segmentation: Blake & Zisserman functional, in: R. Serapioni, F. Tomarelli (Eds.), Variational Methods for Discontinuous Structures, in: Progress in Nonlinear Differential Equations and Their Applications, vol. 25, Birkhäuser, 1996, pp. 57–72.
[13] M. Carriero, A. Leaci, F. Tomarelli, Necessary conditions for extremals of Blake & Zisserman functional, C. R. Math. Acad. Sci. Paris 334 (4) (2002) 343–348.
[14] M. Carriero, A. Leaci, F. Tomarelli, Euler equations for Blake & Zisserman functional, Calc. Var. Partial Differ. Equ. 32 (2008) 81–110, https://doi.org/10.1007/s00526-007-0129-2.
[15] M. Carriero, A. Leaci, F. Tomarelli, A candidate local minimizer of Blake & Zisserman functional, J. Math. Pures Appl. 96 (2011) 58–87, https://doi.org/10.1016/j.matpur.2011.01.005.
[16] M. Carriero, A. Leaci, F. Tomarelli, A survey on Blake–Zisserman functional, Milan J. Math. 83 (2) (2015) 397–420.
[17] M. Carriero, A. Leaci, F. Tomarelli, Segmentation and inpainting of color images, J. Convex Anal. 25 (2018) 435–458.
[18] M. Carriero, A. Leaci, F. Tomarelli, Almansi decomposition of a poly-harmonic function near a crack-tip, J. Convex Anal. 31 (2) (2024) 379–409.
[19] R.H. Chan, A. Lanza, S. Morigi, F. Sgallari, An adaptive strategy for the restoration of textured images using fractional order regularization, Numer. Math., Theory Methods Appl. 6 (1) (2013) 276–296.
[20] T.F. Chan, S. Esedoğlu, Aspects of total variation regularized L1 function approximation, SIAM J. Appl. Math. 65 (5) (2005) 1817–1837.
[21] D. Chen, Y. Chen, D. Xue, Fractional-order total variation image denoising based on proximity algorithm, Appl. Math. Comput. 257 (2015) 537–545.
[22] G.E. Comi, D. Spector, G. Stefani, The fractional variation and the precise representative of $BV^{\alpha,p}$ functions, Fract. Calc. Appl. Anal. (2022).
[23] E. De Giorgi, M. Carriero, A. Leaci, Existence theorem for a minimum problem with free discontinuity set, Arch. Ration. Mech. Anal. 108 (1989) 195–218.
[24] J. Eckstein, D.P. Bertsekas, On the Douglas—Rachford splitting method and the proximal point algorithm for maximal monotone operators, Math. Program. 55 (1992) 293–318.
[25] F. Ferrari, Weyl and Marchaud derivatives: a forgotten history, Mathematics 6 (2018) 6.
[26] A.K. Grünwald, Über “begrentze” Derivationen und deren Anwendung, Z. Angew. Math. Phys. 12 (1867) 441–480.
[27] W. Hinterberger, O. Scherzer, Variational methods on the space of functions of bounded Hessian for convexification and denoising, Computing 76 (2006) 109–133.
[28] F. Kazemi Golbaghi, M.R. Eslahchi, M. Rezghi, Image denoising by a novel variable-order total fractional variation model, Math. Methods Appl. Sci. 44 (2021) 7250–7261.
[29] A. Lanza, A. Leaci, S. Morigi, F. Tomarelli, High order symmetrized fractional variation for signal and image analysis, submitted 2024, in press.
[30] A. Lanza, M. Pragliola, F. Sgallari, Parameter-free restoration of piecewise smooth images, Electron. Trans. Numer. Anal. 59 (2023) 202–229.
[31] A. Lanza, M. Pragliola, F. Sgallari, Residual whiteness principle for parameter-free image restoration, Electron. Trans. Numer. Anal. 53 (2020) 329–351.
[32] A. Lanza, S. Morigi, F. Sgallari, Automatic parameter selection based on residual whiteness for convex non-convex variational restoration, Springer Proc. Math. Stat. 360 (2021) 95–111.
[33] A. Leaci, F. Tomarelli, Bilateral Riemann-Liouville fractional Sobolev spaces, Note Mat. 41 (2) (2021) 61–83.
[34] A. Leaci, F. Tomarelli, Riemann–Liouville fractional Sobolev and bounded variation spaces, Axioms 11 (1) (2022) 30.
[35] A. Leaci, F. Tomarelli, Symmetrized fractional total variation for signal and image analysis, Adv. Cont. Discr. Mod. 14 (2023), https://doi.org/10.1186/s13662-023-03762-8.
[36] A.V. Letnikov, Theory of differentiation of an arbitrary order, Mat. Sb. 3 (1868) 1–68 (in Russian).
[37] H.X. Liang, R. Chan, Truncated fractional-order total variation model for image restoration, J. Oper. Res. Soc. China 7 (4) (2019) 561–578.
[38] S. Morigi, L. Reichel, F. Sgallari, Fractional Tikhonov regularization with a nonlinear penalty term, J. Comput. Appl. Math. 324 (2017) 142–154.
[39] M. Nikolova, Minimizers of cost-functions involving nonsmooth data-fidelity terms. Application to the processing of outliers, SIAM J. Numer. Anal. 40 (3) (2003) 965–994, JSTOR.
[40] M. Nikolova, A variational approach to remove outliers and impulse noise, J. Math. Imaging Vis. 20 (2004) 99–120.
[41] M.D. Ortigueira, F. Coito, From differences to derivatives, Fract. Calc. Appl. Anal. 7 (4) (2004) 459–471.
[42] I. Podlubny, Fractional Differential Equations, Series Mathematics in Science and Engineering, vol. 198, Academic Press, Inc., San Diego, CA, 1999, xxiv+340.
[43] I. Podlubny, Fractional differential equations, Math. Sci. Eng. 198 (1999) 199–221.
[44] Y. Pu, J. Zhou, P. Siarry, N. Zhang, Y. Liu, Fractional partial differential equation: fractional total variation and fractional steepest descent approach-based multiscale denoising model for texture image, Abstr. Appl. Anal. 2013 (2013) 19pp, https://doi.org/10.1155/2013/483791.
[45] Y. Pu, P. Siarry, J. Zhou, N. Zhang, A fractional partial differential equation based multiscale denoising model for texture image, Math. Methods Appl. Sci. 37 (12) (2014) 1784–1806.
[46] D. Lorenz, Q. Tran-Dinh, Non-stationary Douglas–Rachford and alternating direction method of multipliers: adaptive step-sizes and convergence, Comput. Optim. Appl. (2019) 67–92.
[47] L.I. Rudin, S. Osher, E. Fatemi, Nonlinear total variation based noise removal algorithms, Phys. D, Nonlinear Phenom. 60 (14) (1992) 259–268.
[48] S. Samko, A. Kilbas, O. Marichev, Fractional Integrals and Derivatives - Theory and Applications, Gordon and Breach, 1993.
[49] R. Scherer, S.L. Kalla, Y. Tang, J. Huang, The Grünwald–Letnikov method for fractional differential equations, Comput. Math. Appl. 62 (2011) 902–917.
[50] Wenyi Tian, Han Zhou, Weihua Deng, A class of second order difference approximations for solving space fractional diffusion equations, Math. Comput. 84 (294) (2015) 1703–1727.
[51] J. Zhang, K. Chen, A total fractional-order variation model for image restoration with nonhomogeneous boundary conditions and its numerical solution, SIAM J. Imaging Sci. 8 (4) (2015) 2487–2518.